

**Amendment history:**

- [Corrigendum](#) (April 2021)

## APC-activated long non-coding RNA inhibits colorectal carcinoma pathogenesis through reducing exosome production

Feng-Wei Wang, ... , Rui-Hua Xu, Dan Xie

*J Clin Invest.* 2018. <https://doi.org/10.1172/JCI122478>.

**Research** **In-Press Preview** **Gastroenterology** **Oncology**

The adenomatous polyposis coli (APC) gene plays a pivotal role in the pathogenesis of colorectal carcinoma (CRC), but remains a challenge for drug development. Long non-coding RNAs (lncRNAs) are invaluable in identifying cancer pathologies, and providing therapeutic options for cancer patients. Here, we identified a lncRNA (lncRNA-APC1) activated by APC through lncRNA microarray screening, and examined its expression among a large cohort of CRC tissues. A decrease in lncRNA-APC1 expression was positively associated with lymph node and/or distant metastasis, a more advanced clinical stage, as well as a poor prognosis of CRC patients. Additionally, APC can enhance lncRNA-APC1 expression by suppressing the enrichment of PPAR $\alpha$  on the lncRNA-APC1 promoter. Furthermore, enforced lncRNA-APC1 expression was sufficient to inhibit CRC cell growth, metastasis and tumor angiogenesis by suppressing exosome production through directly binding *Rab5b* mRNA and reducing its stability. Importantly, exosomes derived from lncRNA-APC1-silenced CRC cells promoted angiogenesis by activating the MAPK pathway in endothelial cells, and moreover, exosomal Wnt1 largely enhanced CRC cell proliferation and migration through non-canonical Wnt signaling. Collectively, lncRNA-APC1 is a critical lncRNA regulated by APC in the pathogenesis of CRC. Our findings suggest an APC-regulated lncRNA-APC1 program [...]

**Find the latest version:**

<https://jci.me/122478/pdf>



**APC-activated long non-coding RNA inhibits colorectal carcinoma pathogenesis through reducing exosome production**

Feng-Wei Wang<sup>1</sup>, Chen-Hui Cao<sup>1</sup>, Kai Han<sup>1</sup>, Yong-Xiang Zhao<sup>2</sup>, Mu-Yan Cai<sup>1</sup>, Zhi-Cheng Xiang<sup>1</sup>, Jia-Xing Zhang<sup>3</sup>, Jie-Wei Chen<sup>1,4</sup>, Li-Ping Zhong<sup>2</sup>, Yong Huang<sup>2</sup>, Su-Fang Zhou<sup>2</sup>, Xiao-Han Jin<sup>1</sup>, Xin-Yuan Guan<sup>5</sup>, Rui-Hua Xu<sup>1</sup>, Dan Xie<sup>1,2,4</sup>

*<sup>1</sup>Sun Yat-sen University Cancer Center; State Key Laboratory of Oncology in South China; Collaborative Innovation Center for Cancer Medicine, Guangzhou, China,*

*<sup>2</sup>National Center for International Research of Biological Targeting Diagnosis and Therapy; Guangxi Key Laboratory of Biological Targeting Diagnosis and Therapy Research; Collaborative Innovation Center for Targeting Tumor Diagnosis and Therapy, Guangxi Medical University, Nanning, Guangxi, China*

*<sup>3</sup>Department of Oncology, the First Affiliated Hospital, Sun Yat-Sen University, Guangzhou, China.*

*<sup>4</sup>Department of Pathology, Sun Yat-Sen University Cancer Center, Guangzhou, China,*

*<sup>5</sup>Department of Clinical Oncology, the University of Hong Kong, Hong Kong, China.*

Fengwei Wang, Chenhui Cao, Kai Han, Yongxiang Zhao, and Muyan Cai contributed equally to this work.

*Conflict of interest statement: The authors have declared that no conflict of interest exists.*

*Address reprint requests to: Dan Xie, PhD, or Rui-Hua Xu, MD, State Key Laboratory of Oncology in South China, Sun Yat-Sen University Cancer Center, No. 651, Dongfeng Road East, Guangzhou 510060, China. E-mail: [xiedan@sysucc.org.cn](mailto:xiedan@sysucc.org.cn) (D.X.) or [xurh@sysucc.org.cn](mailto:xurh@sysucc.org.cn) (R.H.X.); Tel: 86-20-87343193; fax: +86-20-87343170.*

## **Abstract**

The adenomatous polyposis coli (*APC*) gene plays a pivotal role in the pathogenesis of colorectal carcinoma (CRC), but remains a challenge for drug development. Long non-coding RNAs (lncRNAs) are invaluable in identifying cancer pathologies, and providing therapeutic options for cancer patients. Here, we identified a lncRNA (lncRNA-APC1) activated by APC through lncRNA microarray screening, and examined its expression among a large cohort of CRC tissues. A decrease in lncRNA-APC1 expression was positively associated with lymph node and/or distant metastasis, a more advanced clinical stage, as well as a poor prognosis of CRC patients. Additionally, APC can enhance lncRNA-APC1 expression by suppressing the enrichment of PPAR $\alpha$  on the lncRNA-APC1 promoter. Furthermore, enforced lncRNA-APC1 expression was sufficient to inhibit CRC cell growth, metastasis and tumor angiogenesis by suppressing exosome production through directly binding *Rab5b* mRNA and reducing its stability. Importantly, exosomes derived from lncRNA-APC1-silenced CRC cells promoted angiogenesis by activating the MAPK pathway in endothelial cells, and moreover, exosomal Wnt1 largely enhanced CRC cell proliferation and migration through non-canonical Wnt signaling. Collectively, lncRNA-APC1 is a critical lncRNA regulated by APC in the pathogenesis of CRC. Our findings suggest an APC-regulated lncRNA-APC1 program as an exploitable therapeutic maneuver for CRC patients.

## **Introduction**

As one of the most common human malignancies, colorectal carcinoma (CRC) is a leading cause of cancer-related deaths worldwide. It is well established that the pathogenesis of CRC follows the adenoma-carcinoma sequence and involves multistep tumorigenesis through the progressive accumulation of abnormalities in both tumor-suppressor genes and oncogenes (1, 2). Mutations in the gene adenomatous polyposis coli (APC) play a pivotal role in tumorigenesis and progression of CRC (3). To date, targeting certain oncogenes and their related pathways represents the best option for cancer treatment and improving survival of patients at advanced stages. However, because it is a large scaffold protein with multiple functions, APC remains a challenge to target for translation into drug development.

Long non-coding RNAs (lncRNAs) are a large class of transcripts longer than 200 bases with no protein-coding potential (4). Current research indicates that lncRNAs are exquisitely regulated, and that they can control gene expression to regulate various aspects of biological and/or pathological processes (5, 6). It has been shown that lncRNAs modulate several important cancer phenotypes, including proliferation, apoptosis, immortality, motility, and angiogenesis (7, 8). Due to this, it is now widely understood that lncRNAs are invaluable in their ability to identify cancer pathologies, as well as to provide other prognostic value or even to inform therapeutic options for cancer patients. Despite this, the functions of certain lncRNAs involved in the mediation of APC's anti-cancer role in CRC and any abnormalities

they might possess have yet to be elucidated.

Herein, we used lncRNA microarray screening to identify a lncRNA (TCONS\_00027227) activated by APC through PPAR $\alpha$ , which we named lncRNA-APC1. Examination and function analysis of a large cohort of CRC tissues demonstrated that lncRNA-APC1 plays a crucial tumor suppressive role in the pathogenesis of CRC. Further mechanistic studies revealed that lncRNA-APC1 exerts its function through the direct binding of *Rab5b* mRNA, reducing its stability, and ultimately leading to a decrease in exosome production. This action inhibits the over-activation of the MAPK pathway in endothelial cells, and subsequent suppression of angiogenesis. Importantly, we reveal for the first time, an oncogenic role of CRC-derived exosomal Wnt1 that acts in an autocrine manner through non-canonical Wnt signaling. Collectively, our data uncovered a mechanism of APC signaling in the pathogenic process of CRC, APC/PPAR $\alpha$ /lncRNA-APC1/Rab5b, and revealed the potential for several prognostic and/or therapeutic targets for human CRC.

## Results

### **lncRNA-APC1 is upregulated by APC in CRCs**

Inactivated mutations in the *APC* gene are the initiating mutation driving the tumorigenesis and/or progression of CRC (3). In this study, we set out to investigate the abnormal dynamics and underlying roles of certain lncRNAs that are involved in this process, and applied an lncRNA microarray technique to select and identify which lncRNAs were regulated by APC in CRC cells. We first re-induced wild-type (WT) APC full-length CDS into the SW480 and DLD-1 human CRC cell lines (Figure 1A, B), both of which express an endogenous truncated APC protein (mutated at AAs 1338 and 1427, respectively) that constitutively activates  $\beta$ -catenin/TCF-4 mediated transcription. The two cell lines were examined in two independently repeated microarray tests. We found that 3 lncRNAs were upregulated and 2 lncRNAs were downregulated by a greater than 2-fold induced after ectopic overexpression of WT APC in both lines (Figure 1C, Table 1). Among these, TCONS\_00027227, which we named lncRNA-APC1, is encoded by a gene at chromosome 19p12, and was consistently upregulated by more than 17-fold as examined and confirmed by qRT-PCR (Figure 1D).

Using the 5'- and 3'-RACE assay, we discovered that lncRNA-APC1 was a 1580 nucleotide (nt) intergene transcript and poly (A)-positive. The sequence of full-length lncRNA-APC1 is presented in Supplemental Figure 1 A and C. Northern blot analysis confirmed the size of lncRNA-APC1 in CRC cell lines (Supplemental Figure 1B). Further analysis of the sequences with Open Reading Frame (ORF)

Finder from the National Center for Biotechnology Information failed to predict a protein of more than 55 amino acids (AAs). Additionally, we calculated its coding potential using the Coding Potential Calculator (CPC, <http://cpc.cbi.pku.edu.cn/>) and Coding Potential Assessment Tool (CPAT, <http://cpc.cbi.pku.edu.cn/>). The CPC (using ORF\_ FRAME FINDER) predicted score of lncRNA-APC1 was 36.13, and the CPAT predicted coding probability was 0.008, further supporting that lncRNA-APC1 has no protein-coding potential. Moreover, FISH analysis showed that lncRNA-APC1 was primarily located in the cytoplasm (Figure 1E).

In our study, subsequent qRT-PCR analysis revealed that the expression of lncRNA-APC1 was significantly lower in CRC tissues than that in the 30 cases of corresponding para-normal colorectal tissues (Figure 1F). Furthermore, we tested the expression status of lncRNA-APC1 in 110 cases of CRC tissues and our correlation analysis demonstrated that low expression of lncRNA-APC1 was positively correlated with lymph node and/or distant metastasis of CRC, as well as a more advanced clinical stage ( $P < 0.05$ , Table 2). Kaplan-Meier analysis showed that CRC patients with low levels of lncRNA-APC1 expression had shorter survival times (41.4 months, 95% CI: 36.2-46.7) when compared with patients with normal expression of lncRNA-APC1 (64.3 months, 95% CI: 60.1-68.7) ( $P < 0.001$ , log-rank test, Figure 1G, Table 3). These results indicated that a decrease in lncRNA-APC1, which is downstream of APC, could play an important oncogenic role in the regulation of CRC progression.

**lncRNA-APC1 is regulated by APC through PPAR $\alpha$  in CRC cells**



Previous studies found that truncated APC in CRC cells contributes to tumor cell migration via interacting with the Rac-specific guanine nucleotide exchange factor Asef (9, 10). Hence, we further examined whether mutant APC affects lncRNA-APC1 expression. Two common mutant APC plasmid (gifts from Bert Vogelstein), shown in Supplemental Figure 2A, were transfected into the CRC cell line HCT116 (wild-type APC) respectively (11). Real-time RT-PCR and immunoblot analysis showed that the two APC plasmids produced comparable amounts of APC mRNA and protein (Supplemental Figure 2B, C). Surprisingly, we found that mutant APC331 $\Delta$  has no effect on lncRNA-APC1 expression, APC1309 $\Delta$  mutant overexpression slightly suppressed lncRNA-APC1 expression (Supplemental Figure 2D). In addition, we transfected siRNAs specific for APC into SW480 and DLD-1, and observed similar results (Supplemental Figure 2E, F). These results suggest that wild-type but not truncated APC is mainly responsible for regulating lncRNA-APC1 expression.

It is well accepted that regulating  $\beta$ -catenin stabilization is the most prominent function of APC (12). Therefore, we tested whether or not  $\beta$ -catenin could regulate lncRNA-APC1 expression in CRC. Our results showed that inhibition of  $\beta$ -catenin by specific siRNA resulted in only a slight elevation in the expression of lncRNA-APC1 in the CRC cell lines HCT116 (WT APC,  $\beta$ -catenin mutant) and DLD-1 (Supplemental Figure 3A, B). Consistently, neither wild-type nor mutant  $\beta$ -catenin (45th amino acid deletion mutation in HCT116 or S33Y) overexpression has significant effect on lncRNA-APC1 (Supplemental Figure 3C, D) (11). These

results suggest that  $\beta$ -catenin may be not required for the regulation of lncRNA-APC1 expression by APC.

To further explore the potential mechanisms by which APC regulates lncRNA-APC1 expression, we first analyzed the promoter of lncRNA-APC1. Results from the luciferase reporter assay showed that enforced expression of APC could significantly enhance the transcriptional activity of the lncRNA-APC1 promoter (Figure 2A). To identify which domains might be responsible for the induction of transcriptional activity mediated by APC, we constructed 3 more reporter genes, as indicated in Figure 2B. The data from those assays showed that -160 to -374 bp of the promoter had the most effect on reporter activity (Figure 2C). Further analysis of the transcription factor binding motif by MatInspector software revealed an enrichment for binding motifs of the nuclear receptor PPAR $\alpha$  (peroxisome proliferator-activated receptor) located at -60 to -37 bp (-AAAAGAACTGTGACATACCACAG-) upstream of the lncRNA-APC1 transcription start site (TSS). It has been reported that the PPAR family includes three members, alpha, delta, and gamma, which encode proteins sharing a highly conserved structure and molecular mode of action. PPARs play central roles in the regulation of glucose and lipid homeostasis, and have been shown to be of critical importance in CRC pathogenesis (13, 14). To test whether or not PPAR $\alpha$  regulated lncRNA-APC1 expression, we first transfected siRNAs specific for PPAR $\alpha$  into CRC cells (Figure 2D). We found that lncRNA-APC1 expression was significantly enhanced by PPAR $\alpha$  silencing (Figure 2E), and moreover, the PPAR $\alpha$  binding motif deletion mutation significantly increased the activity of the

lncRNA-APC1 promoter-driven luciferase reporter (Figure 2F). Consistently, the data from dual luciferase reporter assays revealed that enforced expression of PPAR $\alpha$  could abrogate the transcriptional activity of the lncRNA-APC1 promoter induced by APC (Figure 2G, H). Further ChIP analysis confirmed the enrichment of PPAR $\alpha$  binding sites on the promoter of lncRNA-APC1, and that ectopic overexpression of APC substantially suppressed the enrichment of PPAR $\alpha$  on the promoter of lncRNA-APC1 (Figure 2I). However, we did not observe the same altered levels of PPAR $\alpha$  after the enforced expression of APC (data not shown). Together, these findings revealed that APC enhances the expression of lncRNA-APC1 by inhibiting the binding of PPAR $\alpha$  to the promoter of lncRNA-APC1.

### **lncRNA-APC1 suppresses the proliferative and invasive capacities of CRC cells and inhibits angiogenesis**

It is also well established that APC mutations lead to CRC initiation and/or progression by influencing multiple cellular processes, including cell apoptosis, adhesion, and migration, in tumor cells (15). To investigate if lncRNA-APC1 plays an important role in APC-mediated biological functions in CRC, we first stably overexpressed lncRNA-APC1 in DLD-1 and SW480 cells and examined the effect of lncRNA-APC1 on cellular biological functions (Supplemental Figure 4A). The data from these *in vitro* studies showed that ectopic overexpression of lncRNA-APC1 largely inhibited CRC cell proliferation and migration (Figure 3A, B, and Supplemental Figure 4B). Furthermore, *in vivo* assays demonstrated that overexpression of lncRNA-APC1 dramatically inhibited the oncogenic and metastatic

potential of CRC cells in nude mice (Figure 3C-E). Next, to test the contribution of lncRNA-APC1 to APC functions in the pathogenesis of CRC, we stably overexpressed WT APC in the DLD-1 cell line and then stably silenced lncRNA-APC1 expression with specific shRNA (Figure 4A, B). As anticipated, we observed that overexpression of APC significantly inhibited proliferation and migration of CRC cells *in vivo*, and that silence of lncRNA-APC1 in APC-overexpressed CRC cells could largely abrogate the APC-inhibited cell proliferation and migration (Figure 4C, D).

To deepen our understanding of this process, we performed analysis of tumor tissues in a subcutaneous xenograft model, and observed that ectopic overexpression of lncRNA-APC1 led to significant tumor tissue necrosis (almost more than 70% of tumor tissue)(Figure 5A). Although overexpression of lncRNA-APC1 had little effect on CRC cells apoptosis (Supplemental Figure 4C), it did induce cell cycle arrest moderately at the G1 phase (Figure 5B, C). Meanwhile, we found that the expression levels of neither  $\beta$ -catenin nor c-myc (two well-known downstream targets of APC) were influenced by the enforced depletion or overexpression of lncRNA-APC1 (Supplemental Figure 4D). Moreover, T-cell factor/lymphoid enhancer factor (TCF/LEF) reporter gene and c-Myc reporter gene activity assays showed that lncRNA-APC1 has no affection on  $\beta$ -catenin and c-Myc transcription activity (Supplemental Figure 4E). These results suggest that lncRNA-APC1 exerts functions independent on  $\beta$ -catenin or c-Myc. We know that angiogenesis is required to provide the nutrients and oxygen for the survival of tumor cells, and that it is also essential for

their metastasis. We were also able to identify a drastically decreased microvascular density (MVD) in the lncRNA-APC1-overexpressed tumor tissues in our mouse model (Figure 5D), and consistently, our in vitro assays have clearly shown substantially decreased tube formation and migration in HUVECs using exosomes derived from lncRNA-APC1-overexpressed CRC cells (Figure 5E, F).

### **lncRNA-APC1 inhibits angiogenesis by reducing exosome production in CRC cells**

We then asked if lncRNA-APC1 might affect the expression of certain important angiogenesis-associated factors in CRC, including VEGFA, EGF, PDECFG, ANG1, ANG2, and TGF- $\beta$ 1. However, in our study, we did not examine any significant changes in the expression levels in the CRC cells before and after ectopic overexpression of lncRNA-APC1 (Figure 6A). Recently, it has been suggested that exosomes can act as paracrine or autocrine factors to affect important biological functions mediating cell-to-cell interactions (16-18), and further, growing evidence suggests that exosomes released from cancer cells can contribute to tumor angiogenesis and metastasis (19-21). Notably, Irina Nazarenko *et al.* reported that tumor-derived exosomes could efficiently induce angiogenesis without an initial requirement for known angiogenic factors (22). Therefore, in the next part of our study, we isolated exosomes from CRC cell culture medium and confirmed their identity by western blot (Figure 6B) and electron microscopy (Figure 6C). We quantified the size distribution of exosomes using NanoSight analysis (Figure 6D). As shown in Figure 6C, the shape and size distribution of the exosomes in the control

and lncRNA-APC1-overexpressed groups were not significantly different. Surprisingly, the concentrations of the exosome lysates were drastically decreased in the lncRNA-APC1-overexpressed CRC cells as compared to those from the same amount of control cells (Figure 6E); such was confirmed by quantification using NanoSight (Figure 6F). Furthermore, we found that enforced overexpression of APC clearly inhibited the production of exosomes in CRC cells, which could be reversed in part by silence of lncRNA-APC1 (Figure 6G).

We further investigated whether or not lncRNA-APC1 could inhibit tumor angiogenesis through exosomes. We observed that exosomes derived from lncRNA-APC1-overexpressed DLD-1 and SW480 cells yielded a substantial decrease in migration and tube formation of HUVECs when compared to those of the control (Figure 7A, B). Whereas, exosomes derived from lncRNA-APC1-depleted HCT116 cells largely enhanced migration and tube formation of HUVECs (Figure 7C, D). In addition, our immunofluorescence assay demonstrated that exosomes were directly taken-up by HUVECs in vitro (Supplemental Figure 5A) and endothelial cells in vivo (Supplemental Figure 5B). Collectively, these results suggest that lncRNA-APC1 exerts a strong anti-angiogenic effect in CRC cells by suppressing exosome production.

### **lncRNA-APC1 reduces production of CRC exosomes through Rab5b**

Since Ras-related RAB proteins control exosome biogenesis and release (23), we first analyzed the expression levels of certain RAB genes (i.e., *Rab1a*, *Rab5a*, *Rab5b*, *Rab7*, *Rab27a*, *Rab27b*) between the lncRNA-APC1-overexpressed and control CRC

cells. Notably, the mRNA levels of both *Rab5b*, which regulates the motility and fusion of early endosomes, and *Rab27b*, which plays a vital role in exosome release, (24, 25) were significantly decreased with ectopic overexpression of lncRNA-APC1 (Figure 8A). However, since the expression of Rab27b protein was barely detectable in both of our SW480 and DLD-1 cell lines, we thus focused on *Rab5b* in our further studies (Figure 8B). As anticipated, we did observe that lncRNA-APC1 silencing largely prevented the decrease in mRNA and protein levels of *Rab5b* in APC-overexpressed CRC cells (Figure 8C, D). Additionally, neither truncated APC nor  $\beta$ -catenin significantly regulates Rab5b expression (Supplemental Figure 6A-C). To further explore if Rab5b is involved in APC/lncRNA-APC1-mediated cellular functions, we constructed Rab5b stably silenced CRC cells (Figure 8E). We found that silence of Rab5b in DLD-1 cells resulted in an almost 70% decrease in exosomes secretion as determined by NanoSight (Figure 8F). Further in vivo assays showed that knockdown of Rab5b could significantly suppress tumor growth and distant colonization of CRC cells (Figure 8G, Supplemental Figure 6D). Furthermore, we examined the protein expression of Rab5b by IHC in a large cohort of 229 primary CRC tissues. Survival analysis showed that CRC patients with high expression of Rab5b protein had a poorer prognosis than that of patients with low expression of Rab5b (Supplemental Figure 6E, F). These data suggested a critical role of Rab5b in exosome production during CRC cell progression. Subsequently, we tested the contribution of Rab5b to the function of lncRNA-APC1. Our results showed that knockdown of lncRNA-APC1 substantially enhanced in vitro proliferation (Figure

9A, B) and migration (Figure 9C) of CRC cells, an effect that could be markedly prevented by silence of Rab5b.

### **lncRNA-APC1 may interact with *Rab5b* mRNA and reduces its stability in CRC cells**

For the next goal in this study, we were determined to explore the potential mechanisms by which lncRNA-APC1 regulates Rab5b in CRC. It has been established that lncRNAs' ability to recognize complementary sequences allows highly specific interactions that are able to regulate gene expression (4). Many lncRNAs have been reported to function as competing endogenous RNAs (ceRNA) by competitively binding microRNAs or interacting with RNAs directly, thus affecting their stability (7, 8, 26, 27). To test whether or not lncRNA-APC1 regulates *Rab5b* expression by directly interacting with its mRNA, we first compared the mRNA sequences of lncRNA-APC1 and *Rab* family genes using BLAST (<http://blast.ncbi.nlm.nih.gov/>). Surprisingly, we identified two highly complementary regions between lncRNA-APC1 and *Rab5b* mRNA (Figure 10A) and eight highly complementary regions between lncRNA-APC1 and *Rab27b* mRNA (Supplemental Figure 7A), however, this was isolated to *Rab5b* and *Rab27b* mRNA, and no such regions were observed for other *RAB* family genes or *GAPDH* mRNA (data not shown). To validate the direct interaction of lncRNA-APC1 with *Rab5b* mRNA, we mutated two binding sites in lncRNA-APC1 with *Rab5b*, and performed affinity pull-down of endogenous *Rab5b* mRNA using in vitro transcribed biotin-labeled lncRNA-APC1 and lncRNA-APC1-mut (*Rab5b*). The results revealed



that lncRNA-APC1 was significantly enriched in *Rab5b* mRNA compared to that of lncRNA-APC1-mut (*Rab5b*), lncRNA-APC1 antisense control, and *GAPDH* mRNA (Figure 10B). The specific association between lncRNA-APC1 and *Rab5b* mRNA was further validated by our RIP qRT-PCR assay in both SW480 and DLD-1 cells (Figure 10C, D). These findings indicate that lncRNA-APC1 might interact with *Rab5b* mRNA.

Next, to test if lncRNA-APC1 regulates the stability of the *Rab5b* mRNA, we treated DLD-1 and SW480 cells with alpha-amanitin to block RNA-polymerase-II-mediated new RNA synthesis and then measured the loss of *Rab5b* and  $\beta$ -actin over a 24hr period. Ectopic overexpression of lncRNA-APC1, but not that of lncRNA-APC1-mut (*Rab5b*), reduced the half-life of *Rab5b* mRNA (Figure 10E), whereas, knockdown of lncRNA-APC1 clearly elongated the half-life of *Rab5b* mRNA (Supplemental Figure 7B). Moreover, enforced expression of wild-type APC significantly decreased the stability of *Rab5b* mRNA; such could be prevented by silencing lncRNA-APC1 (Supplemental Figure 7C). We further performed rescue functional assay to verify the interaction among APC, lncRNA-APC1 and *Rab5b* in CRC cell line HCT116 (with wild-type APC). As anticipated, ectopic overexpression of wild-type lncRNA-APC1 could suppress APC knockdown-enhanced cell proliferation, cytoskeleton and migration. On the other side, the plasmid containing mutation of *Rab5b* binding sites in lncRNA-APC1 clearly prevented the suppressive affection of wild-type lncRNA-APC1 on CRC cells proliferation, cytoskeleton and migration; such could be substantially rescued by

enforced knockdown of *Rab5b* (Supplemental Figure 8A-D). In addition, a significant inverse correlation between the levels of lncRNA-APC1 and *Rab5b* mRNA was observed in our clinical cohort of 50 cases of CRC tissues (Supplemental Figure 8E). These data, collectively, provided evidences that lncRNA-APC1 could specifically decrease the stability of *Rab5b* mRNA to suppress CRC cells malignant potential; such is dependent on the direct binding of lncRNA-APC1 with *Rab5b* mRNA.

### **Exosomes enhance tumor angiogenesis by activating the MAPK pathway in endothelial cells**

To analyze the mechanisms of lncRNA-APC1 regulated exosomes in regulating tumor angiogenesis, the total RNA of HUVECs incubated with exosomes derived from lncRNA-APC1 silenced or control HCT116 cells was extracted. Next, Gene expression profile microarray was applied to identify the key genes and/or signaling pathways that regulate the functions of HUVECs. Consistent with the exosome-induced functions of HUVECs, Kyoto Encyclopedia Genes and Genomes (KEGG) pathway enrichment analysis of genes potentially regulated by exosomes in our microarray assay revealed significant alternations in regulation of the actin cytoskeleton (Figure 11A), with the greatest enrichment for the signaling pathway of mitogen-activated protein kinase (MAPK). Numerous studies have shown that p38 MAPK cascades are the major signaling pathways involved in regulating endothelial cell actin remodeling, migration, and angiogenesis during cancer progression and metastasis (28-30). To validate the result from the microarray, we first tested the expression of 2 factors, i.e., HSPA6 and PPM1B, both of which can inhibit MAPK

pathway (31-34). Data from qRT-PCR confirmed a significant decrease in expression of both HSPA6 and PPM1B in HUVECs induced with exosomes derived from lncRNA-APC1-silenced HCT116 cells (Figure 11B). Results from western blot assays showed that the p38 MAPK pathway was in fact activated by the exosomes (Figure 11C). Furthermore, knockdown of p38 MAPK largely inhibited tube formation and migration of HUVECs induced by those exosomes (Figure 11D, Supplemental Figure 9A). Actin remodeling is essential for the contractile motion of endothelial cells and angiogenesis (28, 29). Further F-actin staining revealed that stress fiber and lamellipodia were clearly enhanced in CRC cells treated with exosomes, and that such could be successfully halted by silence of p38 (Supplemental Figure 9B).

### **Exosomal Wnt1 enhances proliferation and migration of CRC cells through non-canonical Wnt signaling**

Our study's finding that ectopic lncRNA-APC1 expression can inhibit in vitro CRC cell proliferation and migration, suggests that exosomes may exert their function in an autocrine manner. A previous report has documented that Wnt3A protein is secreted on exosomes and can induce canonical Wnt signaling (35). Therefore, we hypothesized that CRC cell-derived exosomes might exert functions in an autocrine manner by inducing the Wnt pathway. Our immunoblot analysis of CRC cell-derived exosomal lysate showed considerable expression of Wnt1 (Figure 12A). Then, we silenced Wnt1 expression in CRC cells to further explore the function of exosomal Wnt1 (Figure 12B). Meanwhile, we observe no significant changes of lncRNA-APC1

induced by knockdown of Wnt1 (Figure 12C). As shown in the in vitro assay, exosomes derived from Wnt1-silenced CRC cells could, in part, abrogate the enhanced proliferation and migration of the cancer cells that was induced by the control exosomes, indicating that exosomal Wnt1 has signal-inducing activity (Figure 12D-E). However, the levels of T-cell factor/lymphoid enhancer factor (TCF/LEF) reporter activity induced by exosomes derived from CRC cells or Wnt1-silenced CRC cells were comparable (Supplemental Figure 10A), suggesting that exosomal Wnt1 could conduct its function through non-canonical Wnt signaling. We next tested the WNT/PCP signaling which regulates actin cytoskeletal and cell movement (36, 37), as well as the WNT/RTK signaling which activates the PI3K-AKT signaling cascade (38, 39). As anticipated, CRC cell exosomes can largely activate the 3 factors, Rho, JNK (which is involved in WNT/PCP signaling) and AKT, and that such effects can be partly abrogated after depletion of Wnt1 (Supplemental Figure 10B).

## **Discussion**

Mutations in the *APC* gene were reported to occur in up to 80% of sporadic human CRCs (40). Inactivation of *APC* is sufficient to initiate colorectal adenoma in mice, and it is a well-established critical driver of the pathogenic process of CRC (1). Nevertheless, the abnormalities of certain lncRNAs and their roles in mediating the functions of APC in the tumorigenesis and/or progression of CRC have yet to be elucidated.

In the present study, we first used microarray screening to select and identify

lncRNA-APC1 as a downstream factor of APC in CRC. We know that regulation of  $\beta$ -catenin stabilization is the most prominent function of APC, however, results from the  $\beta$ -catenin gene silencing and ectopic expression assay showed that the expression of lncRNA-APC1 was clearly regulated by APC, independently of  $\beta$ -catenin. In addition, we found that wild-type but not truncated APC is mainly responsible for regulating lncRNA-APC1 expression. We performed further biological analysis with the lncRNA-APC1 promoter and the luciferase reporter assay, and our findings indicated that PPAR $\alpha$  might bind with the promoter of lncRNA-APC1 and decrease its transcriptional activity. The PPAR family members play central roles in the regulation of glucose and lipid homeostasis, and they have been shown to be essential in CRC carcinogenesis (14), lending support to the theory that PPAR $\alpha$  is involved in mediating the regulation that occurs between APC and lncRNA-APC1. Furthermore, our PPAR $\alpha$  binding motif deletion reporter and ChIP assays confirmed that PPAR $\alpha$  is responsible for APC-induced lncRNA-APC1 expression.

Subsequently, we investigated the clinical relevance of lncRNA-APC1 and its impact on CRC patients. The results showed that low expression of lncRNA-APC1 in CRC tissues was positively correlated with lymph node and/or distant metastasis of tumors. Moreover, CRC patients with low lncRNA-APC1 expression had a shorter survival time compared to those patients with a normal lncRNA-APC1 expression. These findings suggest that lncRNA-APC1 might play an anti-cancer role in CRC pathogenesis. In order to further our understanding of these concepts, we performed a series of additional *in vitro* and *in vivo* models and loss-of-function assays in this

study. We verified that lncRNA-APC1, functioning as a mediator of APC, was a potent tumor suppressor that could dramatically inhibit the proliferation, growth, and migration of CRC cells in vitro, and substantially suppress tumor formation and distant metastasis in vivo. Interestingly, in a subcutaneous xenograft mouse model we did observe that enforced expression of lncRNA-APC1 in CRC cells led to significant necrosis of tumor tissue. This suggests that, in addition to the moderate cell cycle arrest effect of lncRNA-APC1 in CRC cells, its inhibitory effect on tumor growth in vivo could be the result of other factors, such as the regulation of angiogenesis of CRCs in the tumor microenvironment. As anticipated, we further found that ectopic overexpression of lncRNA-APC1 in CRC cells markedly inhibited tumor angiogenesis both in vitro and in vivo, although certain angiogenic factors were not significantly affected by lncRNA-APC1. It has been reported that tumor-derived exosomes can efficiently induce angiogenesis without the initial requirement for known angiogenic factors (22). We speculated that lncRNA-APC1 might exert its suppressive function through exosomes. Unexpectedly, exosome lysate concentrations measurement and quantitative testing by NanoSight showed that lncRNA-APC1 could substantially suppress the production of exosomes in CRC cells. Furthermore, we found that lncRNA-APC1 was sufficient to inhibit angiogenesis through reducing the levels of exosomes as examined by either in vitro or in vivo assays. These data, taken together, provided sufficient evidence that lncRNA-APC1 reduces exosome production in CRC cells ultimately resulting in the suppression of tumor angiogenesis.

It has been suggested that Ras-related RAB proteins control exosome biogenesis and release (23). Matias Ostrowski and colleagues have previously identified five Rab proteins (Rab2b, Rab9a, Rab5a, Rab27a, and Rab27b) that could influence secretion of exosomes in human HeLa cells (24). Other studies have shown that Rab11 is essential for  $\text{Ca}^{2+}$ -regulated secretion exosomes in an erythroleukemia tumor cell line, and that Rab35 is required for the secretion of proteolipoprotein (PLP)-enriched exosomes by oligodendrocytes (41, 42). Therefore, no consensus has been achieved on which intracellular machinery are involved in exosome production, although it does seem to be dependent on the cell type. In the next parts of our current study, we further identified that Rab5b, a small GTPase protein that regulates the motility and fusion of early endosomes, is a key target of lncRNA-APC1 and is important for the production of exosomes in CRC cells, as evidenced by a group of gain or loss-of-function in vitro and in vivo assays. Furthermore, RIP and RNA pulldown assays verified that lncRNA-APC1 bound the mRNA of *Rab5b* and dramatically decreased its stability, an observation that was also confirmed by examining the correlation between lncRNA-APC1 and Rab5b mRNA expression among our clinical CRC tissues.

Despite all the latest research, the mechanisms by which exosomes induce angiogenesis in CRC remain largely unknown. In recent years, it has been suggested that p38 MAPK cascades are the major signaling pathways that regulate the actin remodeling, migration, and angiogenesis of endothelial cells (28, 30). Consistent with this, our gene expression profile microarray and KEGG analysis indicated that the

MAPK pathway could play a critical role in the angiogenesis process induced by lncRNA-APC1-regulated exosomes. We further demonstrated through loss-of-function in vitro assays that exosomes derived from lncRNA-APC1-silenced CRC cells could enhance the migration, actin remodeling, and angiogenesis of endothelial cells through activation of the MAPK pathway. Exosomes exert their function through transferring their composition, such as protein, microRNA, lncRNA, and circRNA, to recipient cells (18, 43). Clearly, the precise mechanisms by which lncRNA-APC1-regulated exosomes activate the MAPK pathway of endothelial cells need further investigation.

Our in vitro data indicated that the exosomes of CRC cells exert their function in an autocrine manner. Previous research has reported that Wnt protein is secreted on the surface of exosomes (35). Given the well-known role of APC as an essential component of the canonical Wnt pathway (Wnt/ $\beta$ -catenin signaling), we set out to further investigate if lncRNA-APC1, as a key regulator of exosome production and downstream of APC, is involved in the Wnt pathway as it pertains to exosome in CRC. We found that Wnt1 expression on CRC cell-derived exosomes was considerable, and that exosomal Wnt1 substantially enhanced the capacity for CRC cell proliferation and migration through non-canonical Wnt1 signaling. Furthermore, we showed that CRC-derived total exosomes could largely activate the canonical Wnt pathway. However, neither lncRNA-APC1 nor exosomal Wnt1 had any significant effect on the canonical Wnt pathway. Collectively, these data suggested that lncRNA-APC1 might primarily act through suppression of certain subgroups of



exosomes, of which Wnt1<sup>+</sup> exosomes could be an important member.

In summary, this report identifies for the first time that lncRNA-APC1 is an important mediator of APC function through directly regulating *RAB5B* mRNA stability, and thereby reducing exosome production in CRC cells. Moreover, our findings reveal that CRC-derived exosomes exert a strong effect on the pathogenesis and/or angiogenesis of CRC regulated by the lncRNA-APC1/Rab5b axis, suggesting a mechanism for APC signaling, independent of  $\beta$ -catenin and the canonical Wnt pathway (Figure 13). The importance of this result lies in its potential to provide additional targets for therapeutic intervention of human CRC.

## **Methods**

### **Cell culture**

The colorectal cell lines HCT116, DLD-1, SW480, LOVO and SW1116 were from ATCC and all cultured in RPMI 1640 medium with 10% FBS (Invitrogen, Carlsbad, CA, USA). The human kidney HEK293T cell line were from ATCC and cultured in DMEM medium with 10% FBS. The HUVEC cell line was a gift from L.-B. Song (Sun Yat-Sen University Cancer Center, Guangzhou, China) and cultured in SFM medium supplemented with 10% FBS, 0.02  $\mu$ g/ml bFGF, and 0.01  $\mu$ g/ml EGF. Culture conditions were carried out at 37 °C in an incubator (Thermo Fisher Scientific, Waltham, MA, USA) with 5% CO<sub>2</sub>-95% air.

### **Tissue specimens**

A total of 110 primary CRC samples (including 30 adjacent normal tissues) were collected between January 2005 and December 2005 at the Sun Yat-sen University

Cancer Center, Guangzhou, China. The tissue microarray (TAM) containing 229 patients with CRC was constructed as previously reported (44). All of the samples were obtained with informed consent under institutional review board-approved protocols. The CRC cases selected were based on the following inclusion criteria, a clear pathological diagnosis, the presence of follow-up data, and the absence of previous local or systemic treatment. Two pathologists (DX and MYC) reassessed and confirmed all the pathologic diagnosis results. Tumor stage was defined according to the 2002 American Joint Committee on Cancer/International Union Against Cancer tumor-node-metastasis (TNM) classification system. This study was approved by the Institute Research Ethics Committee of Sun Yat-sen University Cancer Center.

### **Microarray analysis**

SW480 and DLD-1 cells were transfected with wild-type (WT) APC, full-length coding sequence (CDS), or control vector. Then, the total RNA was extracted and transcribed. Double-stranded cDNA was labeled using the Quick Amp Labeling kit (Agilent Technologies, Palo Alto, CA) and hybridized to the Arraystar (Rockville, MD) Human 8×60K lncRNA Array v2.0. Following the washing steps, the arrays were scanned by the Agilent Scanner G2505B, and array images were analyzed using the Agilent Feature Extraction software (version 10.7.3.1). Quantile normalization and subsequent data processing were performed using the GeneSpring GX v11.5.1 software (Agilent Technologies). Volcano plot filtering was employed to identify the lncRNAs with statistically significant differences and the threshold to screen

upregulated or downregulated lncRNAs was identified at a fold change  $\geq 1.5$  and a p-value  $\leq 0.05$ .

The gene expression profiles of the HUVEC cells incubated with lncRNA-APC1 silenced or control HCT116 cancer cell-derived exosomes were determined using Phalanx human OneArray microarrays (HOA 6.1) following the manufacturer's instructions.

### **5' and 3' Rapid Amplification of cDNA Ends (RACE)**

The 5'-RACE and 3'-RACE assays were performed to determine the transcriptional initiation and termination sites of lncRNA-APC1 using SuperScript™ IV Reverse Transcriptase (Invitrogen, Carlsbad, CA, USA) in accordance with the manufacturer's instructions.

The primers used for the PCR of the RACE analysis were as follows: 5'-GATGTTCAAGGGCAGGAAGAA-3' (5'RACE) and 5'-TCACAGAAGGCTCTGCGACT-3' (3'RACE).

### **Northern blot**

A biotin-16-dUTP labeled lncRNA-APC1 complementary RNA probe (Sangon biotech, Shanghai, China) and NorthernMax™ Kit (Invitrogen, Carlsbad, CA, USA) were used according to the manufacturers' protocols. Briefly, 10  $\mu$ g total RNA was loaded to the wells of the gel and then run at  $\sim 5$  V/cm. Following the electrophoresis, RNA was transferred to a nylon membrane (GE Healthcare, Little Chalfont, Buckinghamshire, UK) overnight. After 30 min of pre-hybridization, the membrane was hybridized for 16h at 52 °C in ULTRAhyb buffer containing the denatured probe.

After the blocking and washing steps, the membrane was detected using the Chemiluminescent Nucleic Acid Detection Module Kit (Thermo Fisher Scientific, Waltham, MA, USA).

The sequence of the RNA probe was:

5'-biotin-GACUCUCAUACAGGUAGAAGACCCAGGACCCUACCAGUUUACU  
CAAGCC-3'.

### **Fluorescence in situ hybridization**

Paraffin embedded tissues derived from CRC patients' tumors and para-normal colon tissue were used along with a digoxin-LNA-modified oligonucleotide probe (Exiqon, Vedbaek, Denmark) in order to determine the lncRNA location. The slides were mounted onto flow through slide chambers and placed in a hybridization instrument in which the following steps were performed: proteinase-K treatment 15 µg/ml at 37 °C for 8 min, pre-hybridization in hybridization buffer at 37 °C for 30 min, and hybridization with LNA probe (Probe: 5'-DigN-AGCGGGAGAGAAGAGTCACAT-3'-Dig\_N). Stringent washes with 5×SSC, 1×SSC, and 0.2×SSC buffers at 37 °C for 15 min each time were strictly executed. A biotin-SP IgG Fraction Monoclonal Mouse Anti-Digoxin antibody (Jackson ImmunoResearch Laboratories, West Grove, PA, USA) was used to combine with the probe. We used an Alexa Fluor™ 488 Tyramide SuperBoost™ Kit (Invitrogen, Carlsbad, CA, USA) to enlarge the expression signal of the lncRNA-APC1 and stain the nuclei with DAPI (Beyotime, Shanghai, China).

### **Chromatin immunoprecipitation (ChIP)**

The ChIP assay was performed using anti-PPAR $\alpha$ , anti-IgG antibody (R&D Systems, Minneapolis, MN, USA) and the EZ-Magna ChIP™ A/G Chromatin Immuno-precipitation Kit (Merck Millipore, Billerica, MA, USA), according to the manufacturer's instructions. Anti-Mouse IgG was used as a negative control. The strong binding of DNA fragments was detected by real-time PCR using the specific primers.

### **Exosome isolation**

For exosome isolation, cells were maintained in their respective medium with exosome-free FBS, which was prepared by centrifugations in order to remove existing exosomes. Then, exosomes were collected through standard centrifugation steps, as previously described (Théry et al., 2006). Briefly, the collected culture medium was centrifuged at 300  $\times$  g for 10 min, followed by 2000  $\times$  g for 20 min, and then 10000  $\times$  g for 30 min. The supernatant was then filtered through a 0.2- $\mu$ M filter (Pall Corp., Port Washington, NY)). The obtained medium was centrifuged at 100,000  $\times$  g for 70 min at 4 °C to pellet then exosomes. The resulting supernatant was discarded without disturbing the pellet, which was then washed with a large volume of PBS, and then again ultracentrifuged at the same conditions, before final resuspension in a specific volume of PBS. Exosomes were examined by electron microscopy using negative staining, and then quantified using a NanoSight NS300 instrument (Malvern Instruments Ltd. UK) equipped with NTA 3.0 analytical software (Malvern Instruments Ltd. UK) and Micro BCA™ Protein Assay Kit (Thermo Fisher Scientific, Waltham, MA, USA).

## **RNA pull-down**

lncRNA-APC1-mut(Rab5b), lncRNA-APC1, and the negative control lncRNA-APC1 antisense were transcribed *in vitro* from the vectors pSPT19-lncRNA-APC1-mut(Rab5b) and pSPT19-lncRNA-APC1, respectively, using the Biotin RNA Labeling Mix (Roche, Basel, Switzerland), T7 and SP6 RNA polymerase (Promega, Madison, WI, USA). RNA was purified by the RNeasy Mini Kit (Qiagen, Valencia, CA). Then, ~10 pmol of biotinylated RNA from the previous step was added into 200µg of whole-cell lysate from DLD-1 cells and supplemented with tRNA (Ambion, Austin, TX, USA) to a final concentration of 0.1 µg/µL and then incubated at 4 °C overnight with gentle rotation after which 40 µL of prewashed Streptavidin magnetic beads (Invitrogen, Carlsbad, CA, USA) were added for 1h at room temperature. The RNA reserved in the beads was detected by qRT-PCR.

## **RNA immunoprecipitation (RIP)**

pSL-MS2-12x (Addgene) was digested with BamH I and Not I, and the MS2-12x fragment was subcloned into pcDNA3.1, pcDNA3.1-lncRNA-APC1-WT, and pcDNA3.1-lncRNA-APC1-Mut (Rab5b), which were named pcDNA3.1-MS2, pcDNA3.1-MS2-lncRNA-APC1-WT, and pcDNA3.1-MS2-lncRNA-APC1-Mut (Rab5b) respectively. DLD-1 cells were co-transfected with pcDNA3.1-MS2, pcDNA3.1-MS2-lncRNA-APC1-WT, pcDNA3.1-MS2-lncRNA-APC1-Mut (Rab5b), and pMS2-GFP (Addgene). After 48 hours, cells were harvested in order to perform RNA immunoprecipitation (RIP) experiments. IgG and GFP antibody (Abcam,

Cambridge, MA, USA) was used along with the Magna RIP™ RNA-Binding Protein Immunoprecipitation Kit (Millipore, Bedford, MA).

### **Xenograft mouse model**

Athymic nude mice were purchased from Vital River Laboratories (Beijing, China), housed under standard conditions in the animal care facility at the Center of Experimental Animal of Sun Yat-sen University. Treated CRC cancer cells ( $3 \times 10^6$  cells in 0.1 ml of FBS-free culture) were injected subcutaneously into the dorsal flank of 4-5 weeks-old male athymic nude mice (n=8/group). After 4 weeks, mice were sacrificed, and tumors were excised and weighed. For the liver metastasis assays, stable cell lines ( $2 \times 10^6$  cells in 0.05 ml of FBS-free culture) were injected into the spleens of 5-6 week-old male athymic nude mice (n=6/group). The tumor metastatic or distant colonization abilities of the stable cells were determined by intrasplenic injection and tail vein injection models. For lung colonization assays, stable cell lines ( $2 \times 10^6$  cells in 0.1 ml of FBS-free culture) were injected into the tail veins of 5-6 week-old male athymic nude mice (n=6/group). After 6-8 weeks, mice were sacrificed, tissue from liver and/or lung was excised, and the number of tumor nodules formed in the respective organs were counted and analyzed by hematoxylin and eosin staining.

See the Supplemental methods for details on other experimental procedures.

### **Statistical analysis**

For survival analysis, the optimal cut-point for lncRNA-APC1 expression was the median. The correlation between lncRNA-APC1 and the clinicopathological features of CRC patients was analyzed using the  $\chi^2$  test or Fisher's exact test. For univariate survival analysis, survival curves were obtained using the Kaplan-Meier method. The Cox proportional hazards regression model was performed for multivariate survival analysis. Correlation between the relative expression of lncRNA-APC1 and *Rab5b* mRNA was analyzed by using Pearson's correlation. Measurements were analyzed by the independent 2 tailed Student's *t* test or 1-way ANOVA. Statistical significance was defined as a *P* value of less than 0.05.

### **Study approval**

The use of human CRC tissue specimens in this study was approved by the Ethics Committee of Sun Yat-sen University Cancer Center (Guangzhou, China), and written informed consent was obtained from the patients or their guardians before sample collection. All animal studies were approved by the Sun Yat-sen University Institutional Animal Care and Use Committee (Guangzhou, China).

### **Accession numbers**

The Gene Expression Omnibus accession numbers for the lncRNA microarray data for APC overexpressing cell, and gene expression profile microarray data for HUVECs induced by exosomes are GSE113742 and GSE113739, respectively.

### **Author contributions**



D.X. conceived and devised the study. D.X. and F.-W.W designed the experiments and analysis. C.-H. C., K. H., M.-Y. C., J.-X.Z., J.-W.C., Z.-C.X., L.-P.Z., Y.H., S.-F.Z., X.-H.J., and S.-M.L., performed the experiments. M.-Y.C. and Z.-C.X. performed bioinformatics and statistical analysis. F.-W.W, C.-H.C., and K.H. analyzed the data. R.-H.X. Y.-X.Z. and D.X. supervised the research and, together with F.-W.W, C.-H.C., and K. H. wrote the manuscript.

### **Acknowledgments**

This work was supported by grants from the National Key R&D Program of China (No. 2017YFC1309001 and No. 2016YFC1302305), the National Natural Science Foundation of China (grant No. 81430055, 81572359, 81602063, 81730072, 81772595), the Natural Science Foundation of Guangdong (No. S2014030001589), the Doctor start-up project of Natural Science Foundation of Guangdong (2016A030310231), Program for Changjiang Scholars and Innovative Research Team in University of Ministry of Education of China (No. IRT-15R13), and the Guangzhou Science and Technology Plan Projects (Health Medical Collaborative Innovation Program of Guangzhou) (No. 201803040019).

### **References**

1. Markowitz SD, Bertagnolli MM. Molecular origins of cancer: Molecular basis of colorectal cancer. *N Engl J Med* 2009;361:2449-60.
2. Sjoblom T, et al. The consensus coding sequences of human breast and colorectal cancers. *Science* 2006;314:268-74.
3. Nathke I. Cytoskeleton out of the cupboard: colon cancer and cytoskeletal changes induced

- by loss of APC. *Nat Rev Cancer* 2006;6:967-74.
4. Wang KC, Chang HY. Molecular mechanisms of long noncoding RNAs. *Mol Cell* 2011;43:904-14.
  5. Mercer TR, Dinger ME, Mattick JS. Long non-coding RNAs: insights into functions. *Nat Rev Genet* 2009;10:155-9.
  6. Schmitt AM, Chang HY. Long Noncoding RNAs in Cancer Pathways. *Cancer Cell* 2016;29:452-463.
  7. Yuan JH, et al. A long noncoding RNA activated by TGF-beta promotes the invasion-metastasis cascade in hepatocellular carcinoma. *Cancer Cell* 2014;25:666-81.
  8. Cesana M, et al. A long noncoding RNA controls muscle differentiation by functioning as a competing endogenous RNA. *Cell* 2011;147:358-69.
  9. Kawasaki Y, Sato R, Akiyama T. Mutated APC and Asef are involved in the migration of colorectal tumour cells. *Nat Cell Biol.* 2003;5:211-5.
  10. Jiang H, et al. Peptidomimetic inhibitors of APC-Asef interaction block colorectal cancer migration. *Nat Chem Biol.* 2017; 13:994-1001.
  11. Morin PJ, et al. Activation of beta-catenin-Tcf signaling in colon cancer by mutations in beta-catenin or APC. *Science* 1997; 275:1787-90.
  12. Yang J, Zhang W, Evans PM, Chen X, He X, Liu C. Adenomatous polyposis coli (APC) differentially regulates beta-catenin phosphorylation and ubiquitination in colon cancer cells. *J Biol Chem* 2006;281:17751-7.
  13. Seree E, et al. Evidence for a new human CYP1A1 regulation pathway involving PPAR-alpha and 2 PPRE sites. *Gastroenterology* 2004;127:1436-45.
  14. Peters JM, Shah YM, Gonzalez FJ. The role of peroxisome proliferator-activated receptors in carcinogenesis and chemoprevention. *Nat Rev Cancer* 2012;12:181-95.
  15. Preitner N, et al. APC is an RNA-binding protein, and its interactome provides a link to neural development and microtubule assembly. *Cell* 2014;158:368-382.
  16. They C, Zitvogel L, Amigorena S. Exosomes: composition, biogenesis and function. *Nat Rev Immunol* 2002;2:569-79.
  17. Ratajczak J, Wysoczynski M, Hayek F, Janowska-Wieczorek A, Ratajczak MZ. Membrane-derived microvesicles: important and underappreciated mediators of cell-to-cell

- communication. *Leukemia* 2006;20:1487-95.
18. Valadi H, Ekström K, Bossios A, Sjöstrand M, Lee JJ, Lötvall JO. Exosome-mediated transfer of mRNAs and microRNAs is a novel mechanism of genetic exchange between cells. *Nat Cell Biol* 2007;9:654-9.
  19. Iero M, et al. Tumour-released exosomes and their implications in cancer immunity. *Cell Death Differ* 2008;15:80-8.
  20. Zhou W, et al. Cancer-secreted miR-105 destroys vascular endothelial barriers to promote metastasis. *Cancer Cell* 2014;25:501-15.
  21. Hoshino A, et al. Tumour exosome integrins determine organotropic metastasis. *Nature* 2015;527:329-35.
  22. Nazarenko I, et al. Cell surface tetraspanin Tspan8 contributes to molecular pathways of exosome-induced endothelial cell activation. *Cancer Res* 2010;70:1668-78.
  23. Stenmark H. Rab GTPases as coordinators of vesicle traffic. *Nat Rev Mol Cell Biol* 2009;10:513-25.
  24. Ostrowski M, et al. Rab27a and Rab27b control different steps of the exosome secretion pathway. *Nat Cell Biol* 2010;12:19-30; sup pp 1-13.
  25. Yun HJ, et al. An early endosome regulator, Rab5b, is an LRRK2 kinase substrate. *J Biochem* 2015;157:485-95.
  26. Salmena L, Poliseno L, Tay Y, Kats L, Pandolfi PP. A ceRNA hypothesis: the Rosetta Stone of a hidden RNA language? *Cell* 2011;146:353-8.
  27. Tay Y, et al. Coding-independent regulation of the tumor suppressor PTEN by competing endogenous mRNAs. *Cell* 2011;147:344-57.
  28. Rousseau S, Houle F, Landry J, Huot J. p38 MAP kinase activation by vascular endothelial growth factor mediates actin reorganization and cell migration in human endothelial cells. *Oncogene* 1997;15:2169-77.
  29. Kayyali US, Pennella CM, Trujillo C, Villa O, Gaestel M, Hassoun PM. Cytoskeletal changes in hypoxic pulmonary endothelial cells are dependent on MAPK-activated protein kinase MK2. *J Biol Chem* 2002;277:42596-602.
  30. Yoshizuka N, et al. A novel function of p38-regulated/activated kinase in endothelial cell migration and tumor angiogenesis. *Mol Cell Biol* 2012;32:606-18.

31. Huot J, Houle F, Spitz DR, Landry J. HSP27 phosphorylation-mediated resistance against actin fragmentation and cell death induced by oxidative stress. *Cancer Res* 1996;56:273-9.
32. Awano K, et al. Phosphorylation of protein phosphatase 2Czeta by c-Jun NH2-terminal kinase at Ser92 attenuates its phosphatase activity. *Biochemistry* 2008;47:7248-55.
33. Aburai N, Yoshida M, Ohnishi M, Kimura K. Sanguinarine as a potent and specific inhibitor of protein phosphatase 2C in vitro and induces apoptosis via phosphorylation of p38 in HL60 cells. *Biosci Biotechnol Biochem* 2010;74:548-52.
34. Shin SS, et al. HSPA6 augments garlic extract-induced inhibition of proliferation, migration, and invasion of bladder cancer EJ cells; Implication for cell cycle dysregulation, signaling pathway alteration, and transcription factor-associated MMP-9 regulation. *PLoS One* 2017;12:e0171860.
35. Gross JC, Chaudhary V, Bartscherer K, Boutros M. Active Wnt proteins are secreted on exosomes. *Nat Cell Biol* 2012;14:1036-45.
36. Katoh M. WNT/PCP signaling pathway and human cancer (review). *Oncol Rep* 2005;14:1583-8.
37. Johnson R, Halder G. The two faces of Hippo: targeting the Hippo pathway for regenerative medicine and cancer treatment. *Nat Rev Drug Discov* 2014;13:63-79.
38. Yu J, et al. Wnt5a induces ROR1/ROR2 heterooligomerization to enhance leukemia chemotaxis and proliferation. *J Clin Invest* 2016;126:585-98.
39. Anastas JN, et al. WNT5A enhances resistance of melanoma cells to targeted BRAF inhibitors. *J Clin Invest* 2014;124:2877-90.
40. Kinzler KW, Vogelstein B. Lessons from hereditary colorectal cancer. *Cell* 1996;87:159-70.
41. Hales CM, Vaerman JP, Goldenring JR. Rab11 family interacting protein 2 associates with Myosin Vb and regulates plasma membrane recycling. *J Biol Chem* 2002;277:50415-21.
42. Kouranti I, Sachse M, Arouche N, Goud B, Echard A. Rab35 regulates an endocytic recycling pathway essential for the terminal steps of cytokinesis. *Curr Biol* 2006;16:1719-25.
43. Corrado C, Raimondo S, Chiesi A, Ciccia F, De Leo G, Alessandro R. Exosomes as intercellular signaling organelles involved in health and disease: basic science and clinical applications. *Int J Mol Sci* 2013;14:5338-66.
44. Zhu W, et al. Overexpression of EIF5A2 promotes colorectal carcinoma cell aggressiveness by

upregulating MTA1 through C-myc to induce epithelial-mesenchymal transition. *Gut* 2012;  
61:562-75.

## Figures and figure legends

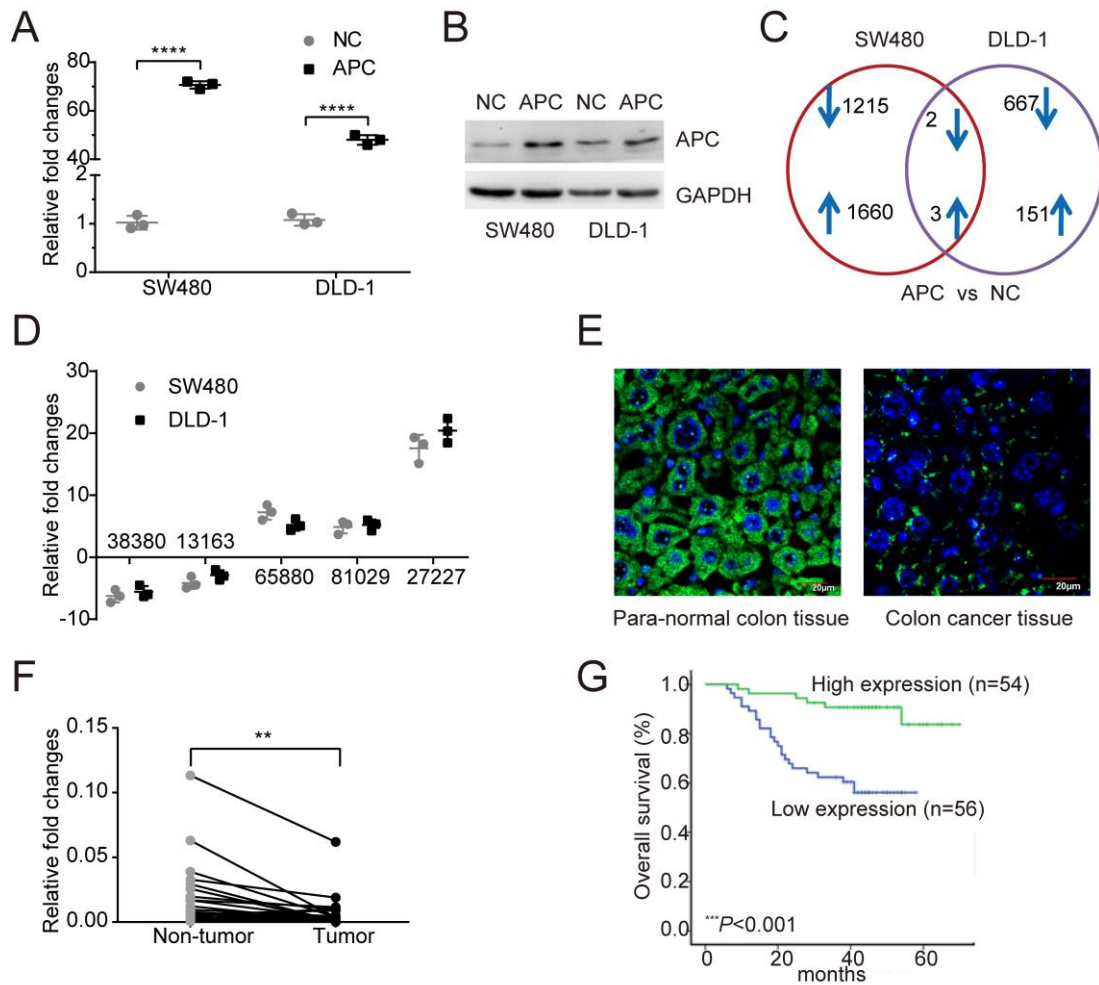


**Figure 1. Upregulation of lncRNA-APC1 by APC.** Expression of APC in indicated cell lines transfected with control or wild-type APC vector as measured by qRT-PCR (**A**) and western blot (**B**). (**C**) Number of altered lncRNAs in indicated cells examined in two independently repeated lncRNA microarray tests. (**D**) qRT-PCR verification of lncRNAs potentially regulated by APC. (**E**) Expression of lncRNA-APC1 was detected by FISH. Data in A, E and F represent the mean  $\pm$  SD of 3 separate experiments. (**F**) Relative expression of lncRNA-APC1 in paired CRC primary tumor tissues and para-normal colon tissues (n=30). (**G**) Kaplan-Meier survival analysis of CRC patients (n=110) according to lncRNA-APC1 expression (cutoff value: median). Experiments in F and G were repeated twice with similar results. \*\* $P < 0.01$ , \*\*\* $P < 0.001$  in independent Student's *t* test (**A** and **F**) and log-rank test (**G**).

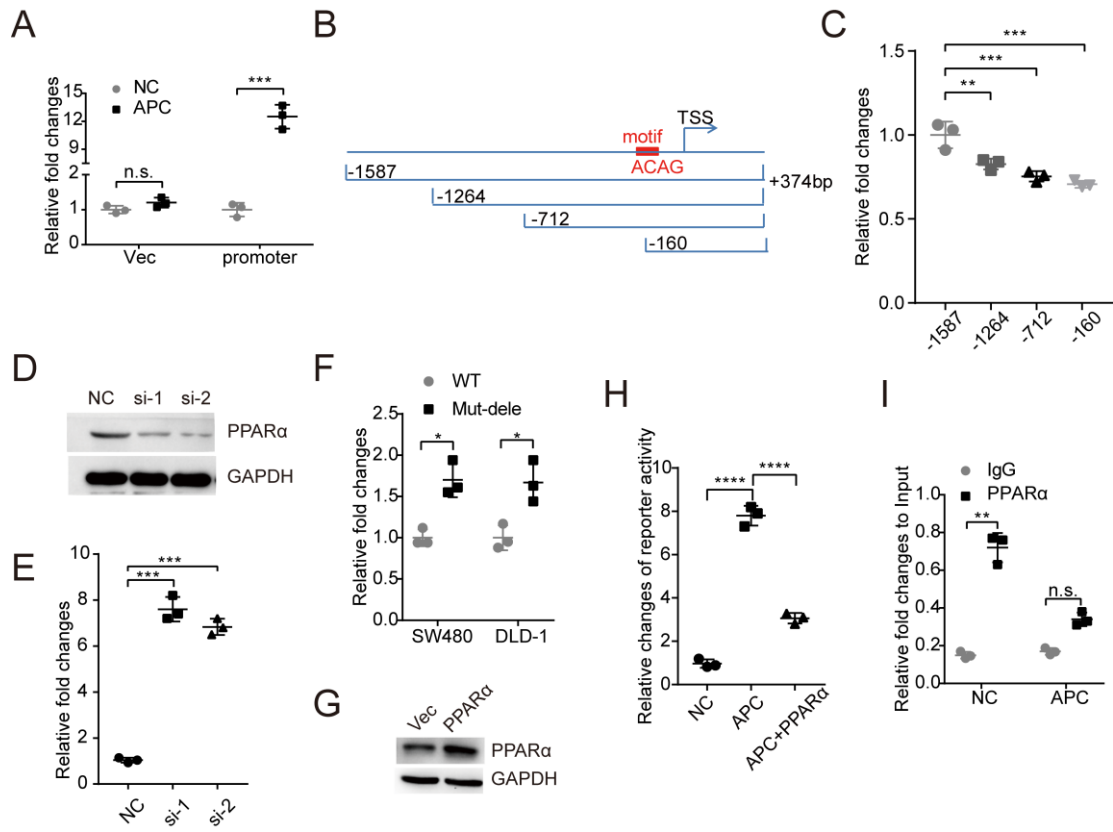


**Figure 2. Upregulation of lncRNA-APC1 by APC is partly dependent on the binding of PPAR $\alpha$  to lncRNA-APC1 promoter.** (A) Luciferase activity of pGL3-lncRNA-APC1 promoter luciferase in DLD-1 cells. (B) and (C), Luciferase activity of indicated pGL3-lncRNA-APC1 promoter luciferase vectors. (D) PPAR $\alpha$  was efficiently knocked down by siRNA detected by western blot. (E) qRT-PCR analysis of the expression of lncRNA-APC1 induced by knocking down of PPAR $\alpha$ . (F) Luciferase activity in indicated cells cotransfected with wild-type (WT) or PPAR $\alpha$  binding motif deletion (Mut-dele) pGL3-lncRNA-APC1 promoter luciferase. (G) Ectopic expression of PPAR $\alpha$  was substantially increased in DLD-1 cells by western blot. (H) Luciferase activity of lncRNA-APC1 promoter cotransfected with APC or/and PPAR $\alpha$  construct. (I) Analysis by ChIP assay to detect the enrichment of PPAR $\alpha$  on the promoter of lncRNA-APC1. All luciferase data has been normalized relative to Renilla luciferase activity. Data represent the mean  $\pm$ SD of 3 separate experiments. All experiments were repeated at least 3 times. \* $P$ <0.05, \*\* $P$ <0.01, \*\*\* $P$ <0.001 in independent Student's  $t$  test or 1-way ANOVA (C, E, and H).

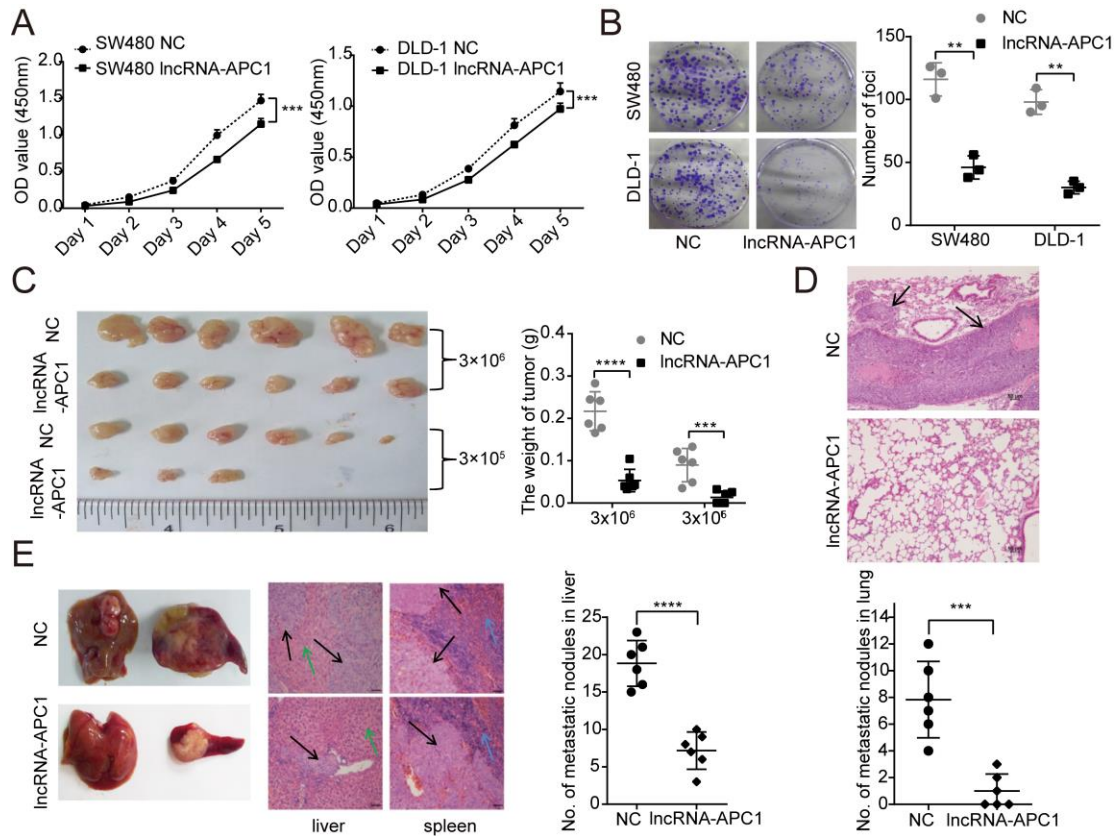


**Figure 3. Suppression of CRC tumorigenesis and metastasis by lncRNA-APC1.**

(A) The rate of cell proliferation of empty vector or lncRNA-APC1 transfected cells by CCK8 assay ( $P < 0.05$ ). (B) Representative images of decreased foci formation. (C) Images of xenograft tumors formed in nude mice. (D) Representative images of H&E-stained sections derived from metastatic nodules in the lung (original magnification, 100x). (E) Representative images of liver and spleen tissue in nude mouse metastasis model. Black arrow: CRC cells, Green arrow: liver tissue, Blue arrow: spleen tissue (original magnification, 100x). Error bars represent mean  $\pm$  SD from 3 independent experiments. Scale bars: 50  $\mu$ m. \*  $P < 0.05$ , \*\*  $P < 0.01$ , \*\*\*  $P < 0.001$ , \*\*\*\*  $P < 0.0001$  in independent Student's *t* test.



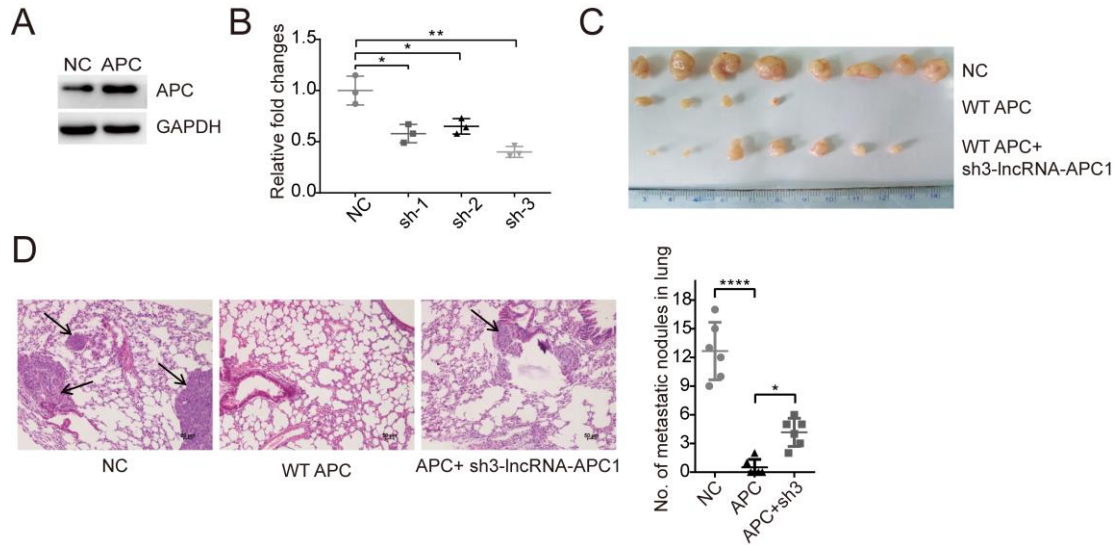


**Figure 4. The function APC exerts is partly dependent on lncRNA-APC1.** (A) APC expression in the DLD-1 stable cell line. (B) Relative expression of lncRNA-APC1 in DLD-1 cells transfected with shRNA specific for silencing lncRNA-APC1 from 3 independent experiments. Error bars represent mean $\pm$ SD from 3 independent experiments. (C) Images of the xenograft tumors formed in nude mice. (D) Representative images of H&E-stained sections derived from metastatic nodules in the lung (original magnification, 100x). Scale bars: 50 $\mu$ m. \* $P$ <0.05, \*\* $P$ <0.01, \*\*\*\* $P$ <0.0001 in 1-way ANOVA.

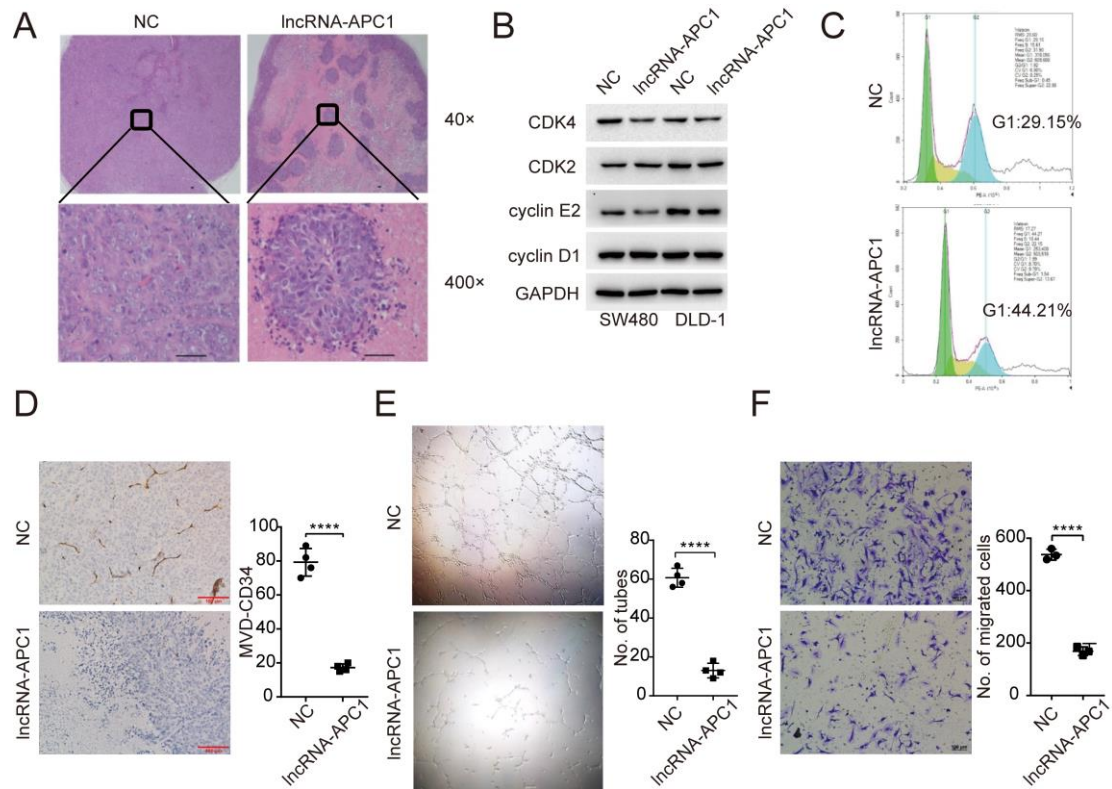


**Figure 5. Suppression of CRC cell tumor growth by lncRNA-APC1 acts through the inhibition of tumor angiogenesis.** (A) Representative images of H&E-stained sections derived from xenograft tumors formed in nude mice. (B) Expression of cell cycle checkpoint marker as examined by western blot. (C) Flow cytometry analysis of cell cycle. (D) MVD of indicated xenograft tumors detected by CD34 staining. Capillary tube formation assay (E) and transwell invasion assay (F) of HUVECs treated by indicated exosomes derived from transfected HCT116 cells ( $**** P < 0.0001$  in independent Student's *t* test). Error bars represent mean  $\pm$  SD from 3 independent experiments in E and F.

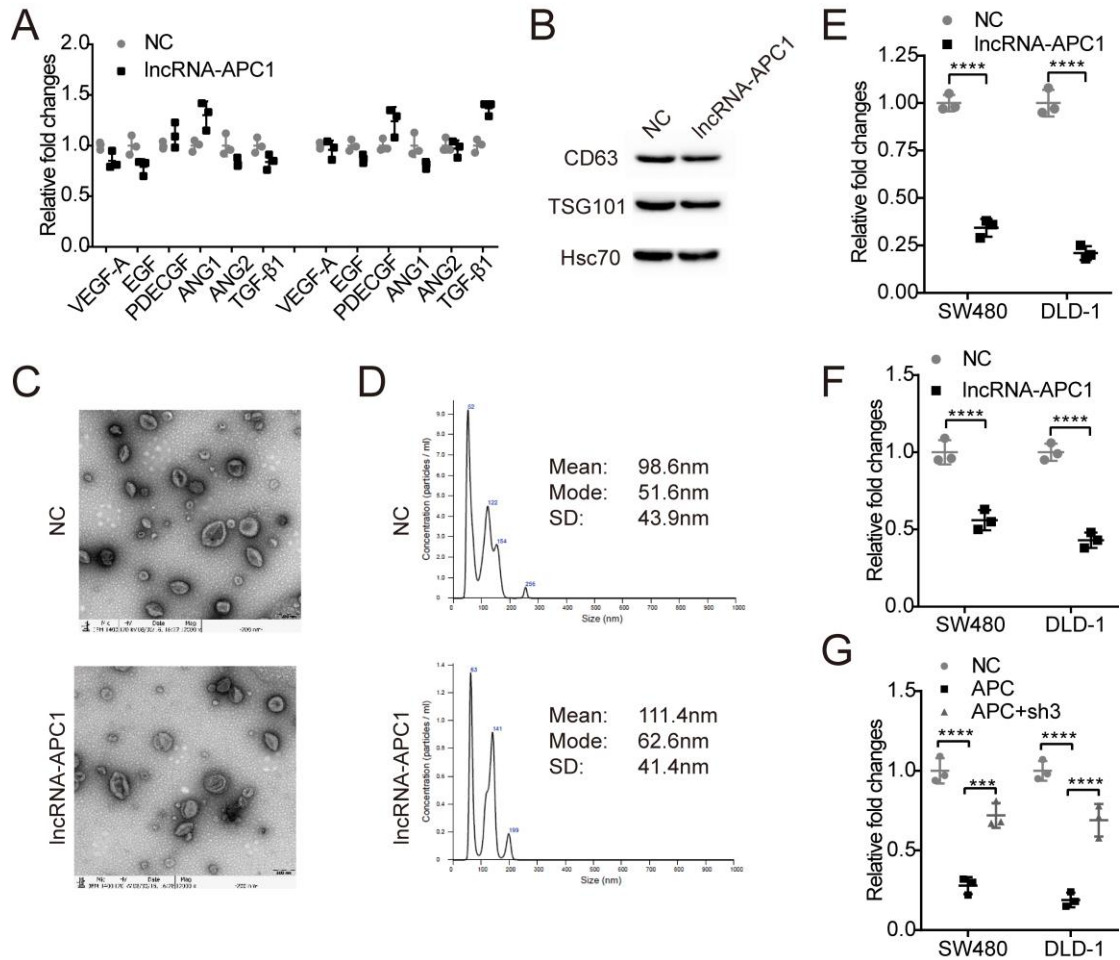


**Figure 6. IncRNA-APC1 suppresses exosomes production.** (A) Relative expression of angiogenesis-associated factors in cells stably overexpressing IncRNA-APC1 or control cells. (B) Western blotting analysis of exosome markers. (C) Representative images of exosomes by electron microscopy detection. (D) Size distribution of exosomes analyzed by NanoSight. Relative fold changes in protein concentrations of exosome lysates as examined by BCA assay (E) or (F) NanoSight. (G) Relative fold changes of in protein concentrations of exosome lysates as examined by BCA assay. All experiments were repeated at least 3 times. Error bars represent mean $\pm$ SD from 3 independent experiments. \*\*\* $P$ <0.001, \*\*\*\* $P$ <0.0001, in independent Student's  $t$  test or 1-way ANOVA (G).

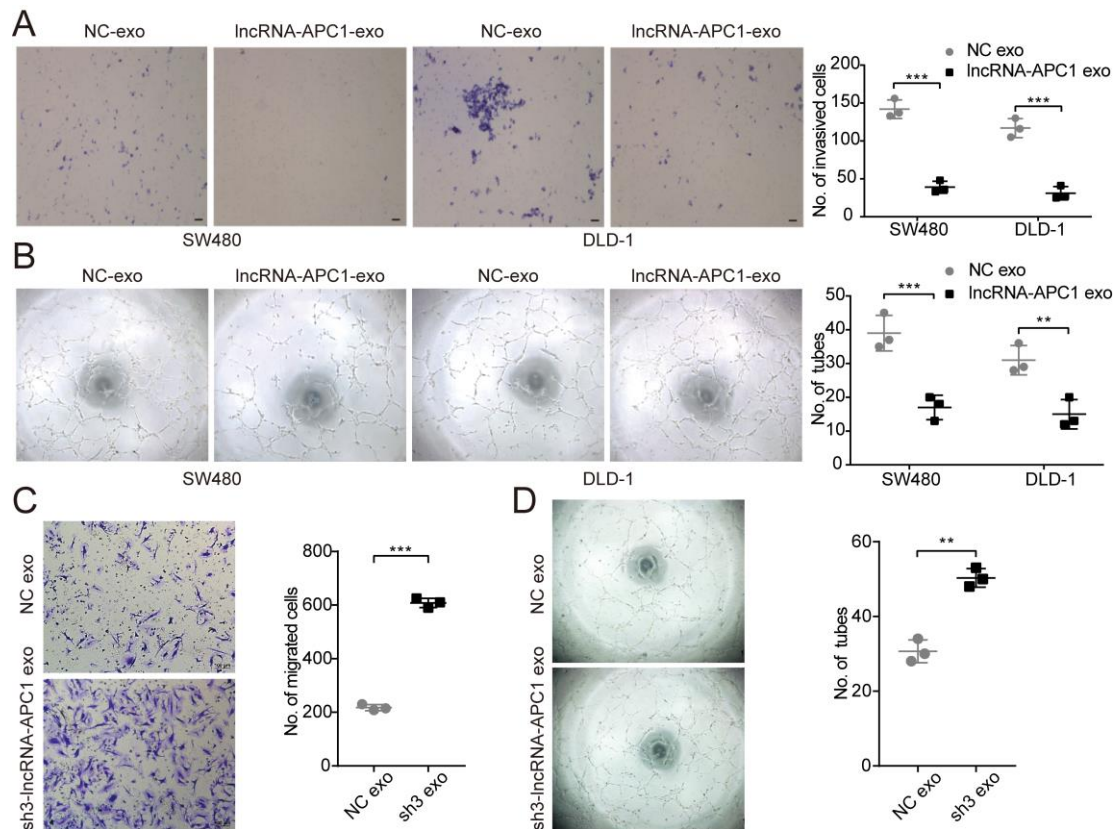


**Figure 7. lncRNA-APC1 inhibits tumor angiogenesis through exosomes. (A)** Transwell invasion assay of HUVECs treated by indicated exosomes ( $P < 0.01$  in independent Student  $t$  test). **(B)** Capillary tube formation assay of HUVECs treated by indicated exosomes. **(C)** Transwell invasion assay of HUVECs treated by indicated exosomes derived from transfected HCT116 cells. **(D)** Capillary tube formation assay of HUVECs treated by indicated exosomes. Error bars represent mean  $\pm$  SD from 3 independent experiments. \*\*  $P < 0.01$ , \*\*\*  $P < 0.001$ , in independent Student's  $t$  test.

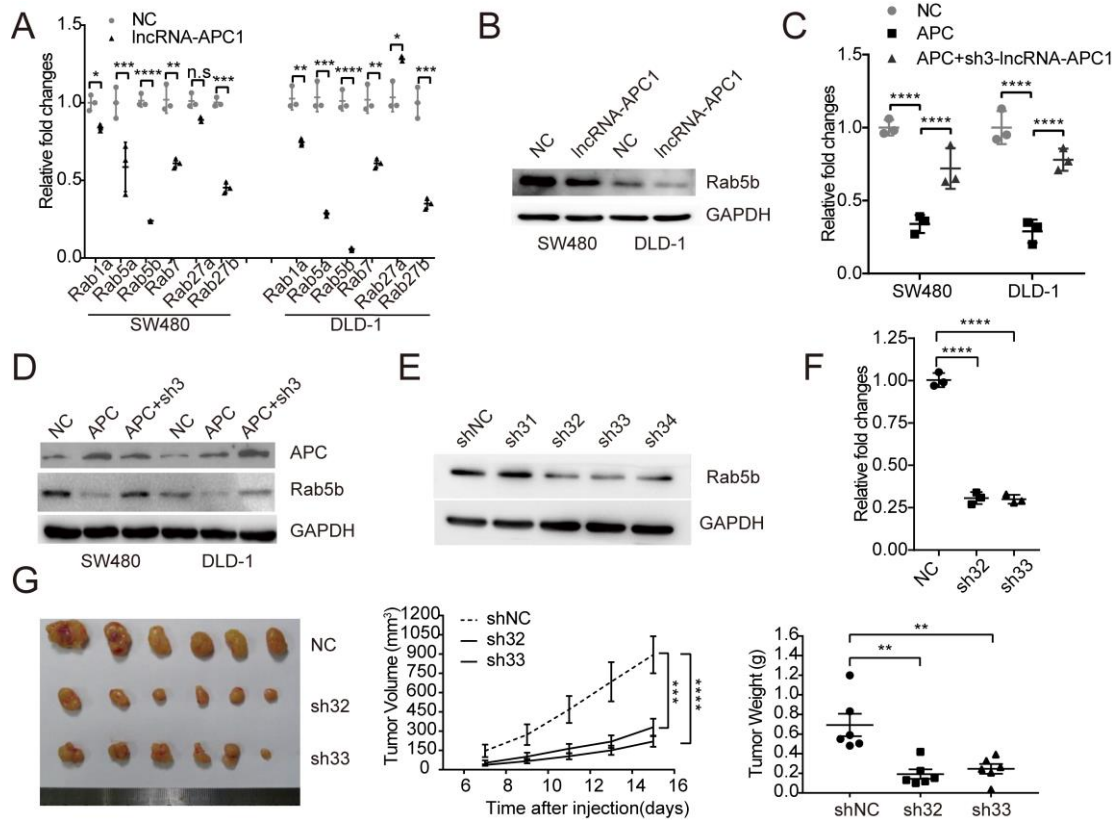


**Figure 8. IncRNA-APC1 reduces the production of CRC exosomes through Rab5b.** (A) qRT-PCR shows the relative expression of *RAB* genes. (B) Rab5b expression in indicated IncRNA-APC1 stable or control cells detected as by western blot. Levels of Rab5b mRNA (C) and protein (D) in indicated cells. (E) Rab5b was efficiently knocked down by specific shRNA. (F) Relative fold change in protein concentration of exosomes lysates as examined by BCA assay. (G) Images of the xenograft tumors formed in nude mice by injecting Rab5b stable silenced or control cells. Error bars represent mean $\pm$ SD from 3 independent experiments. \*\* $P < 0.01$ , \*\*\* $P < 0.001$ , \*\*\*\* $P < 0.0001$  in independent Student's *t* test (A) or 1-way ANOVA.

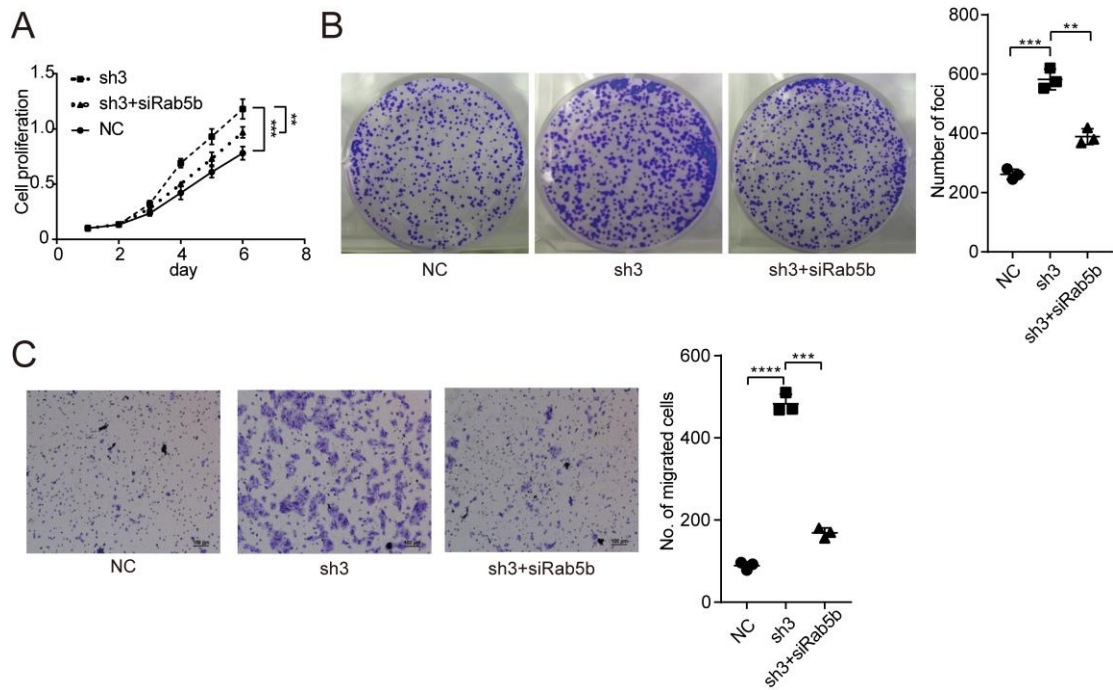


**Figure 9. IncRNA-APC1 silencing enhanced proliferation and migration of CRC cells through Rab5b.** (A) The cell proliferation rate induced by IncRNA-APC1 silencing and/or Rab5b knock down, as determined by CCK8 assay. (B) Representative images of foci formation. (C) Representative images of transwell invasion assay. Error bars represent mean $\pm$ SD from 3 independent experiments. \*\* $P$ <0.01, \*\*\* $P$ <0.001, \*\*\*\* $P$ <0.0001 in 1-way ANOVA.

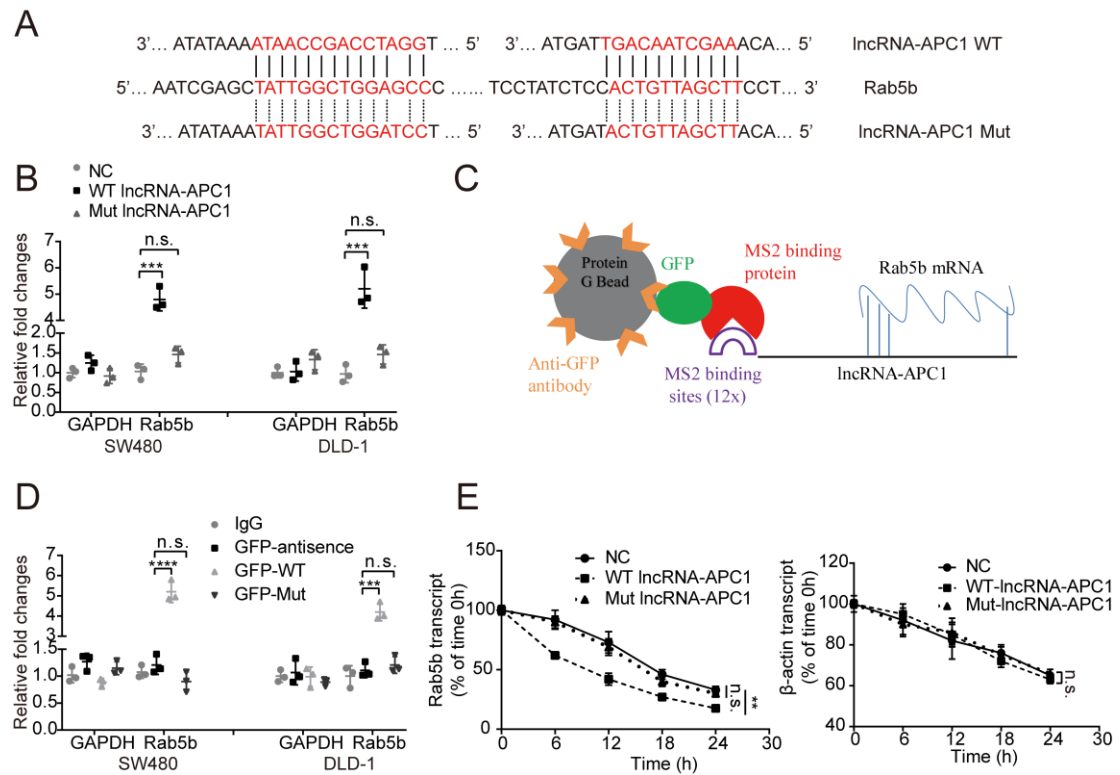


**Figure 10. In CRC cells, lncRNA-APC1 interacts with and reduces the stability of *Rab5b* mRNA.** (A) Regions of putative binding between *Rab5b* mRNA (Query) and lncRNA-APC1 (subject). (B) SW480 and DLD-1 cell lysates were incubated with biotin-labeled wild-type (WT) or mutant type (Mut) lncRNA-APC1; after pull-down, mRNA was extracted and tested by qRT-PCR. (C) Model of RIP assay. (D) RIP-derived RNA was examined by qRT-PCR. The level of qRT-PCR products has been normalized relative to input RNA and IgG control. (E) The stability of *Rab5b* mRNA and beta-actin mRNA was measured by qRT-PCR relative to time 0 after blocking new RNA synthesis with alpha-amanitin and normalized to 18S rRNA. Error bars represent mean  $\pm$  SD from 3 independent experiments. \*\* $P < 0.01$ , \*\*\* $P < 0.001$ , \*\*\*\* $P < 0.0001$  in 1-way ANOVA. n.s.: no significant difference.

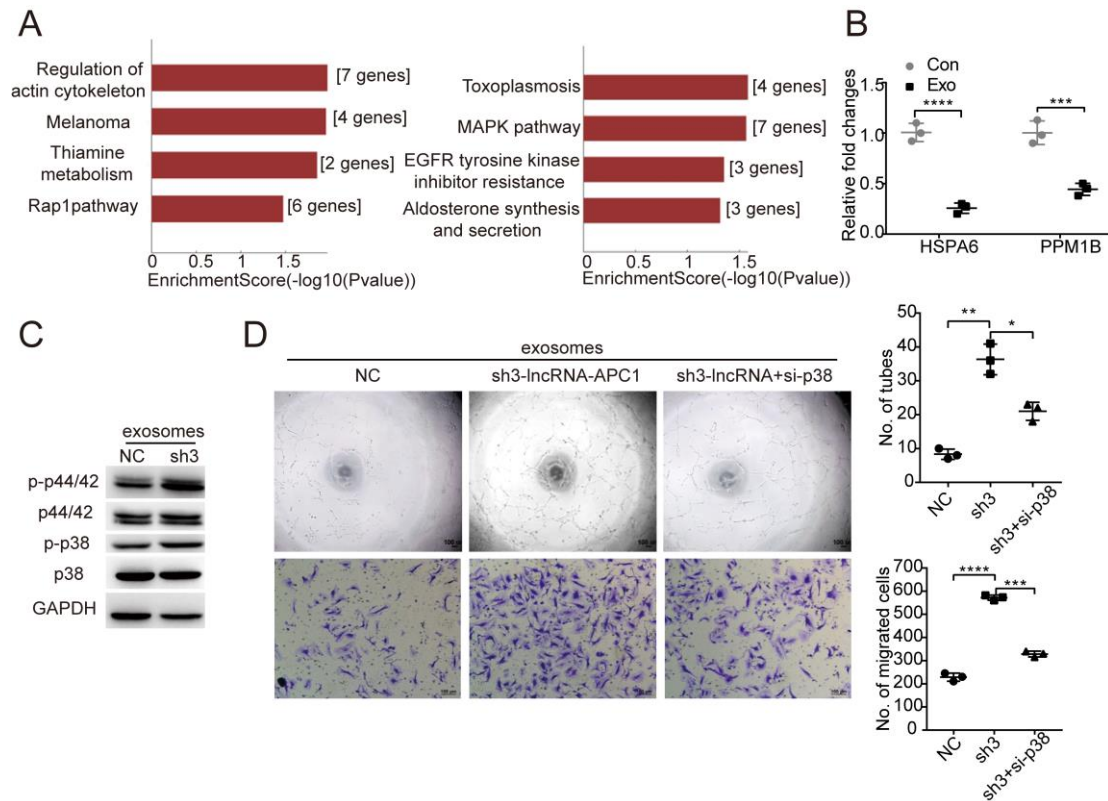


**Figure 11. Exosomes enhance tumor angiogenesis by activating MAPK signaling of HUVECs.** (A) Function (left) and pathway (right) enrichment analysis of the result from the gene expression profile microarray. (B) Relative expression of indicated genes examined by qRT-PCR. (C) Western blot assay shows that the MAPK pathway in HUVECs was activated by exosomes derived from lncRNA-APC1 silenced HCT116 cells. (D) Capillary tube formation (up) and transwell invasion assay (down) of HUVECs treated by indicated exosomes ( $P < 0.05$  in independent Student  $t$  test). The capillary tube formation experiment was performed at least 3 times independently from the assay in Figure 7D. Error bars represent mean  $\pm$  SD from 3 independent experiments. \*  $P < 0.05$ , \*\*  $P < 0.01$ , \*\*\*  $P < 0.001$ , \*\*\*\*  $P < 0.001$  in independent Student's  $t$  test or 1-way ANOVA (D).



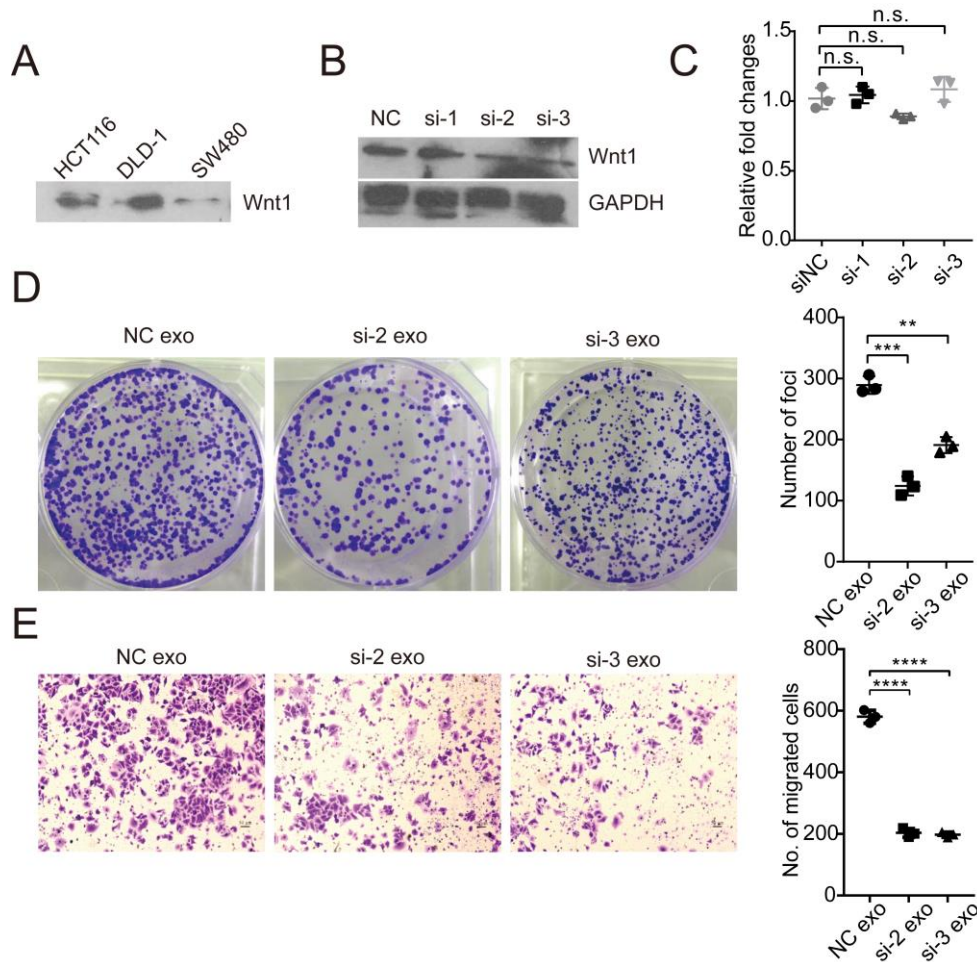


**Figure 12. Exosomal Wnt1 enhances CRC cell proliferation and migration through non-canonical Wnt signaling.** (A) Wnt1 expression in indicated cells derived exosomes. (B) Wnt1 expression was effectively knocked down by specific siRNA-2 and siRNA-3. (C) Expression of lncRNA-APC1 detected by qRT-PCR. (D) Representative images of decreased foci formation induced by Wnt1 silencing exosomes. (E) Representative images of transwell invasion assay. Error bars represent mean  $\pm$  SD from 3 independent experiments. \*\* $P < 0.01$ , \*\*\* $P < 0.001$ , \*\*\*\* $P < 0.001$  in 1-way ANOVA. n.s.: no significant difference.

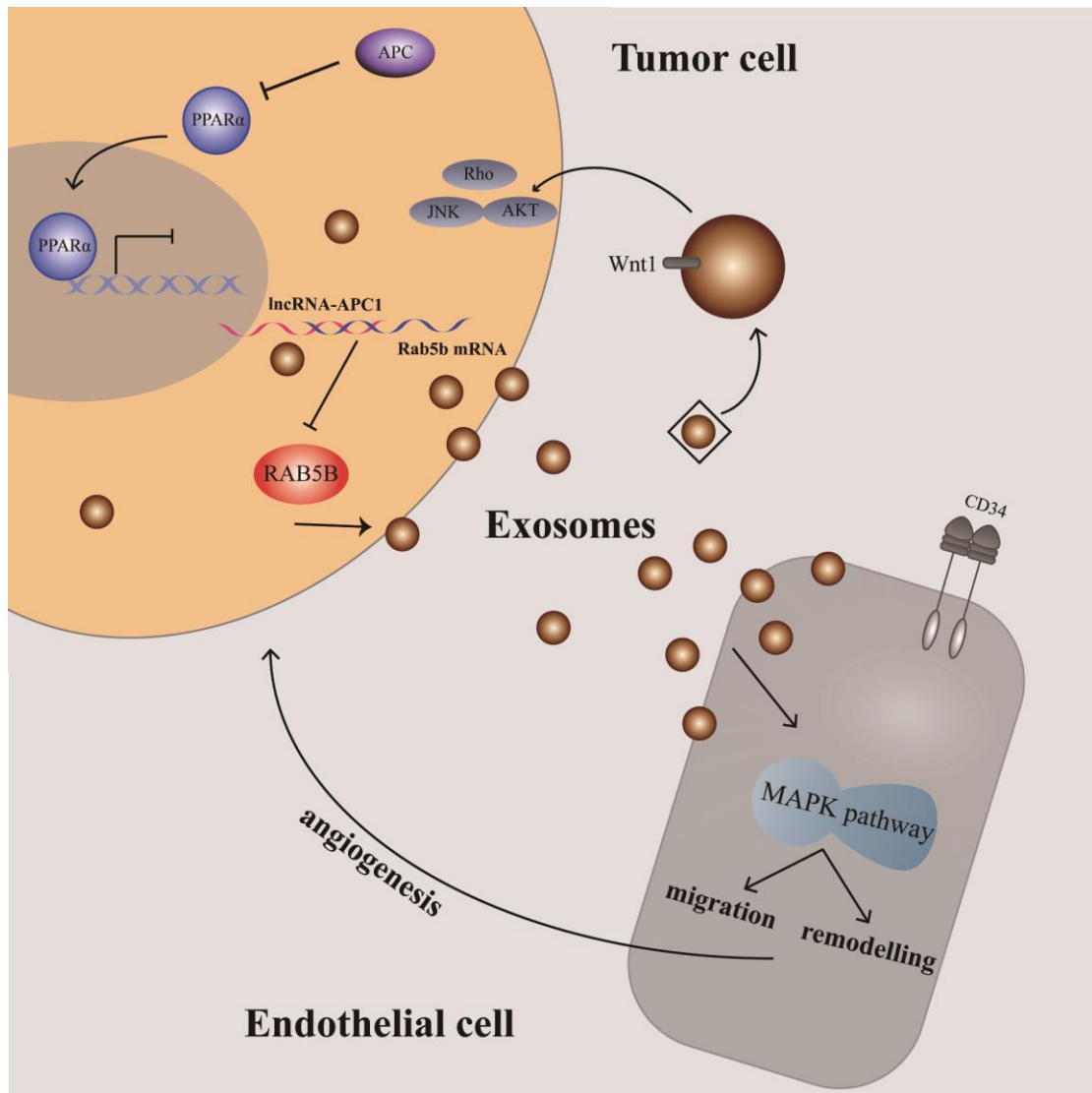


**Figure 13. Model of lncRNA-APC1 functions and mechanisms during CRC pathogenesis.**

**Table 1 lncRNAs regulated by ectopic APC expression in both SW480 and DLD-1 cell lines.**

Fold	change	seqname	genesample
-2.3660802	Down	ENST00000538380	AC091878.1
-3.5207261	Down	TCONS_00013163	XLOC_006432
3.5765904	Up	ENST00000465880	RP11-80H8.4
2.5030724	Up	ENST00000581029	RP11-838N2.4
6.7291048	Up	TCONS_00027227	XLOC_013265

**Table 2 Relationship between lncRNA-APC1 expression level and clinical pathological parameters of CRC**

Variable	Number of cases	LncRNA-APC1 expression		<i>p</i> *
		High expression	Low expression	
Age, yr		54	56	
>60 <sup>a</sup>	51	26	25	
≤60	59	28	31	0.712
Gender				
Female	53	27	26	
Male	57	27	30	0.708
Tumour location				
Colon	66	32	34	
Rectum	44	22	22	0.876
Histological grade(WHO)				
G1-2	87	45	42	
G3	23	9	14	0.283
pT status				
T1-T2	29	21	8	
T3-T4	81	33	48	0.003
Clinical stage				
I+II	42	15	27	
III+IV	68	39	29	0.027
Lymph node status				
No metastasis	42	15	27	
Metastasis	68	39	29	0.027
CEA level				
< 5(μg/L)	69	33	36	
> 5(μg/L)	41	21	20	0.731

<sup>a</sup> mean age; CRC, colorectal carcinoma; CEA, carcino-embryonic antigen; \*  $\chi^2$  test

**Table 3 . Univariate and multivariate Cox regression analysis of different prognostic variables in patients of colorectal cancer**

Variable	Subset	Hazard ratio for DSS (95% CI)	P value
<b>Univariate analysis (n=110)</b>			
Age ( yr )	≤ 60 <sup>a</sup> vs. >60	1.470 (0.717-3.014)	0.293
Gender	Male vs. Female	0.712 (0.343-1.479)	0.363
Tumor location	Colon vs. Rectum	0.598 (0.274-1.307)	0.198
Histological (WHO)	grade G1-2 vs. G3	2.907(1.381-6.116)	0.005
Clinical stage	I+II vs. III+IV	2.648 (1.277-5.490)	0.009
pT status	T1+2 vs. T3+4	4.174(1.258-13.845)	0.020
pN status	N0 vs. N1	2.648 (1.277-5.490)	0.009
CEA level	< 5(μg/L) vs. > 5(μg/L)	1.615 (0.788-3.311)	0.190
lncRNA-APC1 expression level	Low expression vs. High expression	0.198 (0.081-0.487)	<0.001
<b>Multivariate analysis (n=110)</b>			
Histological (WHO)	grade G1-2 vs. G3	2.319 (1.084-4.959)	0.030
pT status	T1+2 vs. T3+4	2.046(0.581-7.208)	0.265
pN status	N0 vs. N1	1.764(0.833-3.733)	0.138
lncRNA-APC1 expression level	Low expression vs. High expression	0.253 (0.101-0.632)	0.003

<sup>a</sup> mean age; CRC, colorectal carcinoma; CEA, carcino-embryonic antigen;